Contents lists available at ScienceDirect

Chemical Engineering Research and Design

journal homepage: www.elsevier.com/locate/cherd

A shortcut design method for complex distillation structures

*Fanyi Duanmu, Dian Ning Chia, Eva Sorensen**

Department of Chemical Engineering, University College London, Torrington Place, London WC1E 7JE, United Kingdom

ARTICLE INFO

Article history:
Received 15 December 2021
Received in revised form 6 February 2022
Accepted 22 February 2022
Available online 25 February 2022

Keywords:
Distillation
Design
Shortcut method
Optimisation
Dividing wall column

ABSTRACT

Distillation is by far the most common fluid separation method in the chemical industry, and its design is routinely conducted using commercial design software, often based on initial shortcut calculations. Whilst simulation and optimisation of simple distillation systems are fairly straightforward, the design of more complex structures, such as dividing wall columns (DWC), can prove problematic due to failure to initialise or to converge, and no adequate shortcut methods exists for these structures. In this work, a novel shortcut method is presented which can solve the shortcut design problem simultaneously also for complex structures using a simple optimisation procedure without the need for iterative manual calculations. The method is illustrated by four case studies. The shortcut design variables obtained using this method can be used to initialise rigorous simulation or optimisation problems, thus greatly reducing the risk of initialisation failure or convergence issues, also for very complex structures.

1. Introduction

Distillation is one of the most technically mature and most widely used separation methods in the chemical industry. As distillation is a very energy intensive process, proper design and operation is essential to reduce cost and environmental impact. Rigorous simulation and optimisation of distillation columns is routinely carried out as part of the design procedure, or to study the potential of new designs or structures. For complex structures, however, finding a good initial guess for the design from which to start a simulation or optimisation can sometimes be quite challenging, particularly for structures such as dividing wall columns (DWC) or other highly integrated systems. A proper shortcut design method is therefore essential in order to obtain a set of initial values to be used in rigorous simulations, and good initial values found by shortcut methods can also reduce the convergence difficulty and time taken for rigorous optimisation (Dejanović et al., 2010b; Urselmann et al., 2011; Skiborowski et al., 2015; Tsatse et al., 2021).

The main variables associated with a distillation column are variables related to the design, mainly total number of stages and stream locations, as well as variables related to the operating specifications, mainly reflux/boilup ratio, heat input, distillate/bottom flowrates, and potential sidedraw stream flowrates (Sorensen, 2014). Shortcut methods are usually used to find two key variables, the minimum reflux ratio and the minimum number of stages, from which the other parameters are then derived. These key variables are also a rough indication of the operating cost and capital cost, respectively.

1.1. Shortcut methods for conventional column systems

Shortcut methods for design of conventional distillation column systems can be categorised into graphical methods and equation based methods. One of the earliest, and still most popular, graphical shortcut methods is the McCabe–Thiele method (McCabe and Thiele, 1925). This method utilises the vapour–liquid equilibrium (VLE) diagram, the so-called *x*–*y*

* *Corresponding author.*
E-mail address: e.sorensen@ucl.ac.uk (E. Sorensen).
https://doi.org/10.1016/j.cherd.2022.02.026

Nomenclature

Symbols

A_e	area of equipment e (m^2)
D_i	internal diameter of column (in.)
D_o	outer diameter of column (in.)
E	fractional weld efficiency (–)
f_{lang}	Lang factor (–)
f_m	material factor (–)
F_s	total molar flowrate of stream s ($kmol\,h^{-1}$)
K_i	K-value of component i (–)
L	column height (in.)
$N^{c,p}$	number of stages in section p of column c (–)
N^c_{feed}	feed stage of column c (–)
$N^{c,p}_{min}$	minimum number of stages in section p of column c (–)
N_{sl}	liquid sidedraw stage (–)
N_{sv}	vapour sidedraw stage (–)
N_s	sidedraw stage (–)
P	total pressure (Pa)
P_d	design pressure of column (psig)
p_i	partial pressure of component i (Pa)
P_o	operating pressure of column (psig)
$P_{sat,i}$	saturated vapour pressure of component i (Pa)
q	feed state (–)
Q_e	heat duty of equipment e (kW)
$r_1/r_2/r_3$	radius of column section 1, 2, or 3, refer Fig. C1 (m)
R_d	main column distillate distribution ratio (–)
R_{sl}	liquid split ratio (–)
R_{sv}	vapour split ratio (–)
RR^c	molar reflux ratio of column c (–)
RR^c_{min}	minimum molar reflux ratio of column c (–)
S	maximum allowable stress for the column shell (psi)
S_{pv}	pinch variable set (–)
T	temperature (K)
ΔT_e	minimum temperature difference for equipment e (K)
$t_{payback}$	payback period (y)
t_p	thickness of shell to withstand pressure (in.)
t_s	average thickness of shell (in.)
t_w	thickness of shell to withstand wind and earthquake (in.)
U_e	heat transfer coefficient of equipment e ($kW\,m^{-2}\,K^{-1}$)
W_{shell}	weight of column shell (lb)
$x_{s,i}$	liquid molar composition of component i in stream s ($mol\,mol^{-1}$)
$y_{s,i}$	vapour molar composition of component i in stream s ($mol\,mol^{-1}$)
Z	objective function defined in the shortcut method (–)
z_i	feed molar composition of component i ($mol\,mol^{-1}$)

Greek letters

α_{ij}	relative volatility of component i in terms of component j (–)
$\Delta^{c,p}_j$	pinch variable j in section p of column c (–)
ρ_{shell}	density of column shell material ($lb\,in.^{-3}$)

Superscrpits

bot	bottom section of the column shortcut structure
C1/C2/C3	column 1, 2, or 3
main	main column
mid	middle section of the column shortcut structure
pre	prefractionator column
top	top section of the column shortcut structure
C	condenser
R	reboiler

Subscrpits

b	bottom stream
d	distillate stream
feed	feed stream
feedL	liquid phase of feed stream
feedV	vapour phase of feed stream
hk	heavy key component
lb	lower bound
lk	light key component
N	number of stages
s	sidedraw stream
sl	side liquid stream
spec	design specification
sv	side vapour stream
tc	thermal coupling stream
ub	upper bound
CAPEX	Capital Expenditure
CEPCI	Chemical Engineering Plant Cost Index
OPEX	Operating Expenditure

Abbreviations

DoF	degree of freedom
DWC	dividing wall column
FUGK	Fenske–Underwood-Gilliland–Kirkbride
GA	genetic algorithm
MINLP	mixed integer non-linear programming
NLP	non-linear programming
OAERAP	outer approximation/equality relaxation/augmented penalty
PWLA	piecewise linear approximating
RVT-DWC	reduced vapour transfer dividing wall column
TAC	total annualised cost
VLE	vapour–liquid equilibrium

diagram, with the assumption of constant molar overflow introduced by Lewis (1909) to avoid the use of an energy balance. The minimum reflux ratio can be obtained with the assumption of infinite number of stages. Then, with a fixed reflux ratio, the operating lines (representing the mass balances) can be constructed in the diagram, and the number of equilibrium stages and the feed location can be visualised and found from the diagram. The McCabe–Thiele method can also be applied for columns with multiple feed streams and/or sidedraw streams. Originally, this method could only be used for binary systems, but Hengstebeck (1946) extended the McCabe-Thiele method to multi-component mixtures by reducing a multi-component mixture into a pseudo-binary mixture, which increased the applicability of the McCabe–Thiele method. Kong and Maravelias (2019)

further developed the McCabe–Thiele method based on a programming approach. They replaced the *x*–*y* diagram with a VLE model where the diagram was split into continuous piecewise linear approximating (PWLA) functions. Two different strategies were introduced to find the minimum reflux ratio depending on the existence of the concave behaviour in the VLE model. The minimum number of stages and the optimal feed location was found by optimisation using a model with material balance equations and the relevant composition constraints. The method was claimed to be more flexible compared to the original McCabe–Thiele method, however, the requirement of continuous PWLA functions and optimisation greatly increased the complexity.

Instead of using simplifying assumptions in relation to energy, Smith (1963) utilised the enthalpy-concentration diagram method proposed by Ponchon and Savarit to generate their shortcut design. Their method could provide more accurate predictions, but additional information, such as calorimetric data and the relevant enthalpy calculations, was required. Later, Gani and Bek-Pedersen (2000) proposed a shortcut method based on the use of a driving force diagram (a graph of driving force against liquid/vapour composition) suitable also for multi-component mixtures and for azeotropic mixtures. The diagram is always concave for both zeotropic and azeotropic mixtures, for the latter in the form of two connected concave curves, and the minimum reflux ratio was obtained from the slope of the operating lines passing through the peak. The number of stages was counted similarly to for the McCabe-Thiele method and the optimal feed location was calculated from a proposed equation.

Although graphical methods are easy to understand, they are not applicable for actual design, and with the development of computer programming, equation-based methods became preferred to avoid the tedium of redrawing figures (Perry and Green, 2008). The most famous and classical equation-based shortcut method is the Fenske–Underwood–Gilliland–Kirkbride (FUGK) method. The Fenske equation (Fenske, 1932) is applied to obtain the minimum number of stages required at total reflux. The average relative volatility used in the equation may, however, leads to an underestimation of the minimum number of stages if the difference between the top and bottom relative volatilities is large. Thus, splitting a column into two sections (rectifying and stripping sections) can give a more accurate result and the feed location can then also be obtained (Towler and Sinnott, 2007). The Underwood equations (Underwood, 1949) are widely used for determining the minimum reflux ratio with the assumption of infinite number of stages and constant relative volatility. The key concept is to find the common root in the equation proposed by the author, which is then used to find the minimum reflux ratio. With known values of minimum number of stages, minimum reflux ratio, and actual reflux ratio, the empirical correlation diagram proposed by Gilliland (1940) can be used to obtain the actual number of stages. Finally, the feed stage can be calculated by the Kirkbride equation (Kirkbride, 1944). Alternatively, with a split column design as mentioned above, the feed location, or the ratio between feed location and total number of stages, can also be obtained using the Fenske equation with the feed stage composition treated as the feed composition. Thus, using only the FUG equations is also applicable. The FUGK method is easy to construct and can provide a good initial start for simulation of both binary and multicomponent systems.

There are other shortcut methods aiming to find only one or some of the values needed for a shortcut design and these methods are often used to replace the corresponding parts of the McCabe–Thiele or FUGK methods to provide a more accurate prediction. Smoker's equation (Smoker, 1938) can be used to determine the number of stages with the assumption of constant molar overflow and constant relative volatility for binary systems. This method can be used in conjunction with the McCabe–Thiele method when the relative volatility is close to one, as the number of stages will then be large and it is difficult to draw and count these stages on the *x*–*y* diagram. The Smoker equation was later simplified by Jafarey et al. (1979) to obtain only the first root through an approximate analytical solution, and then extended by Bandyopadhyay (2006) to remove the assumption of constant molar overflow. Winn (1958) proposed a method for calculating the total number of stages using the equilibrium constant, *K*, instead of the relative volatility and their method is often used to replace Fenske's equation for more accurate prediction when the relative volatility is sensitive to temperature. Seedat et al. (2020) proposed a novel graphical method to obtain the number of stages required at total reflux by plotting contours of the vapour-liquid equilibrium (VLE) on the *x*–*y* diagram and counting the "stairs" between the VLE and $x = y$ lines, through an equation relating the vapour composition of a component to its liquid composition with a component ratio defined in the paper.

Other methods have been proposed which are used to find only the reflux/boilup ratios. Glinos and Malone (1984) extended the Underwood equations for the sharp/non-sharp separation of multi-component mixtures into algebraic equations to find the minimum reflux ratio. Chou et al. (1986) proposed a factor method to find the minimum reflux ratio for a multiple feed distillation column, where an equation to calculate the contribution of the feed streams to the minimum reflux ratio was introduced.

1.2. *Shortcut methods for complex column systems*

The methods mentioned above are limited to conventional columns, and they cannot be used, or need to be modified or extended, for the case of more complex column designs such as dividing wall columns (DWC). Triantafyllou and Smith (1992) extended the application of the FUGK method to suit the DWC. The DWC was modelled based on a Petlyuk design, with three separate column sections (one column section for the prefractionator, or feed side of the dividing wall, and two column sections for the main column, above and below the side stream location), then the FUGK method was applied to each section, and the number of stages on either side of the dividing wall was equalised by adjusting the reflux ratio in the prefractionator. Muralikrishna et al. (2002) proposed a similar method, but instead of providing just one solution, their work used a visualisation method to demonstrate all the possible column designs. A figure showing all feasible designs was generated by analysing seven flowrate constraints in the system with fixed reflux ratio in the prefractionator, and then converting the constraints into a 2D figure whose axes are the flowrates of the two components in the "net distillate" from the prefractionator. In addition, equi-cost curves (in terms of constant total number of stages) and equi-energy curves (in terms of constant vapour flowrate in the bottom column) were plotted in the figure to assist the designer in exploring

the effects of the design parameters on the associated cost and energy.

Instead of using the FUGK method, Sotudeh and Hashemi Shahraki (2007) proposed a method based only on the Underwood's equation. In their design, the DWC was again modelled as a Petlyuk design, with the main column split into two sections at the sidedraw location. The highest reflux ratio out of the three sections was chosen as the minimum reflux ratio. After finding this, the other key parameters, such as the number of stages, stream locations, and internal split ratios, were calculated based on the equations provided in the paper.

Amminudin and Smith (2001) proposed a semi-rigorous shortcut design for a DWC by using the equilibrium stage composition concept, which was initially used for analysing azeotropic separations (Van Dongen and Doherty, 1985; Castillo et al., 1998). Unlike the other methods, this method did not assume constant relative volatility but utilised the stage liquid composition profile method proposed by Castillo et al. (1998) to find the intersection point between the rectifying and stripping sections. In this way, the compositions and locations of the thermal coupling streams could be identified.

Halvorsen (2001) proposed an effective and relatively simple visualisation method for finding the minimum total vapour flow in the DWC called the V_{min} method. The V_{min} method is based only on the Underwood equations and is plotted based on the calculated minimum vapour flow and distillate flow in each column section (*y*-axis as normalised minimum vapour flow and *x*-axis as normalised feed distribution, which is the distribution of feed components to the products). The V_{min} diagram clearly shows the vapour and liquid traffic in each column section, which helps with the initial design of a DWC. The peak points in the diagram represent the minimum theoretical energy required to achieve the separation task in each column section, and the highest point represents the energy needed to achieve the minimum total energy requirement of a DWC (which is also the energy needed for the most difficult separation of the binary pair in the feed mixture). It should be noted that the V_{min} method cannot be used individually to yield all the initial design parameters for a DWC, but the Fenske's equation can be used in addition to determine the minimum number of stages. All stream flowrates and compositions necessary to perform Fenske's equation can be calculated by simple mass balances with information collected from the V_{min} diagram. Ränger and Grützner (2021) extended the V_{min} diagram into a stage-adapted V_{min} diagram by introducing a factor *n*, which is a ratio between the actual number of stages divided by the corresponding minimum number of stages obtained by Fenske's equation. Then, a pareto-optimal design between minimum number of stages and minimum energy requirement can be obtained through a heuristic rule proposed in the literature. It was claimed that the design obtained from the stage-adapted V_{min} diagram can yield better product purities, and can be used for multiple dividing wall column with finite number of stages.

To conclude, most, if not all, of the methods summarised above cannot be applied to complex structures without modifications of key steps. Even for the FUGK method, which can be used for both conventional designs and simple DWCs, an additional iterative procedure is required to meet the wall stage requirement in the DWC which is imposed to ensure that the pressure drops on either side of the wall is equal. For a complex column structure, especially for design with additional constraints other than product specifications, currently available shortcut methods are usually solved in multiple steps sequentially and/or in an iterative procedure, which may require significant manual effort.

This paper thus aims to develop a novel shortcut method which can be used for both simple and complex distillation column structures, which properly handles any constraints imposed by the different structures and solves the shortcut design simultaneously without the need for repetitive procedures. The methodology is described in Section 2 using a simple conventional distillation column as an illustrative example. Then, in Section 3, the proposed shortcut method is applied to different complex column structures to show the adaptability and performance of the method, including different types of DWCs with both traditional and novel flow patterns. Next, and to show the accuracy of the method, some of the results from the shortcut method are compared to their equivalent optimised designs found via rigorous optimisation in Section 4. Finally, Section 5 highlights the key findings of this work and provides directions for future work.

2. Shortcut design methodology

The shortcut method proposed in this work determines all the design variables simultaneously, which ensures that the final solution is true for the whole set of design equations. The method involves optimising an equation set based on an objective function which minimises mixing effects at the feed location, and possibly other special constraint(s), e.g. same number of stages on both sides of the wall in a dividing wall column (represented by Δ_N in this work, see details in Section 3), which is merged into the objective function. In this way, the special constraint(s) can be fulfilled while minimising the mixing effect. More importantly, the proposed shortcut method does not involve any manual iterative procedures and is therefore far less demanding in terms of manual effort and computation time than current shortcut methods. The optimisation procedure used is simple and can easily be implemented in Matlab, or even Excel. It will be shown that the method is highly efficient, yet very accurate, and can be used for both simple and complex column configurations with excellent results.

In this work, the concept of the pinch point, first introduced by Colburn (1941), is one of the main assumptions utilised to determine the shortcut design. Generally, there will be a stage or location in the column where the pinch point occurs, i.e. the composition changes are negligible for both liquid and vapour streams entering and leaving the stage. This stage is determined as the feed location in the proposed shortcut method as the energy lost due to mixing effects will be at its minimum at this location. Other main assumptions utilised are constant molar overflow and steady state conditions, which eliminates the energy balances and differential equations, respectively, making the shortcut model consist of only algebraic equations describing the mass balances. In principle, the proposed shortcut method can be used for both constant or changing relative volatility models, equally for both ideal or non-ideal liquid models. However, to reduce the complexity of the algebraic equations used, constant relative volatility at the feed condition and an ideal model is used for the case studies shown in this work. These assumptions may lead to deviations for systems with large changes in relative volatilities or for thermally coupled designs (Dejanović et al., 2010b), for which a more detailed approach that takes into account variations in relative volatility can be used if needed.

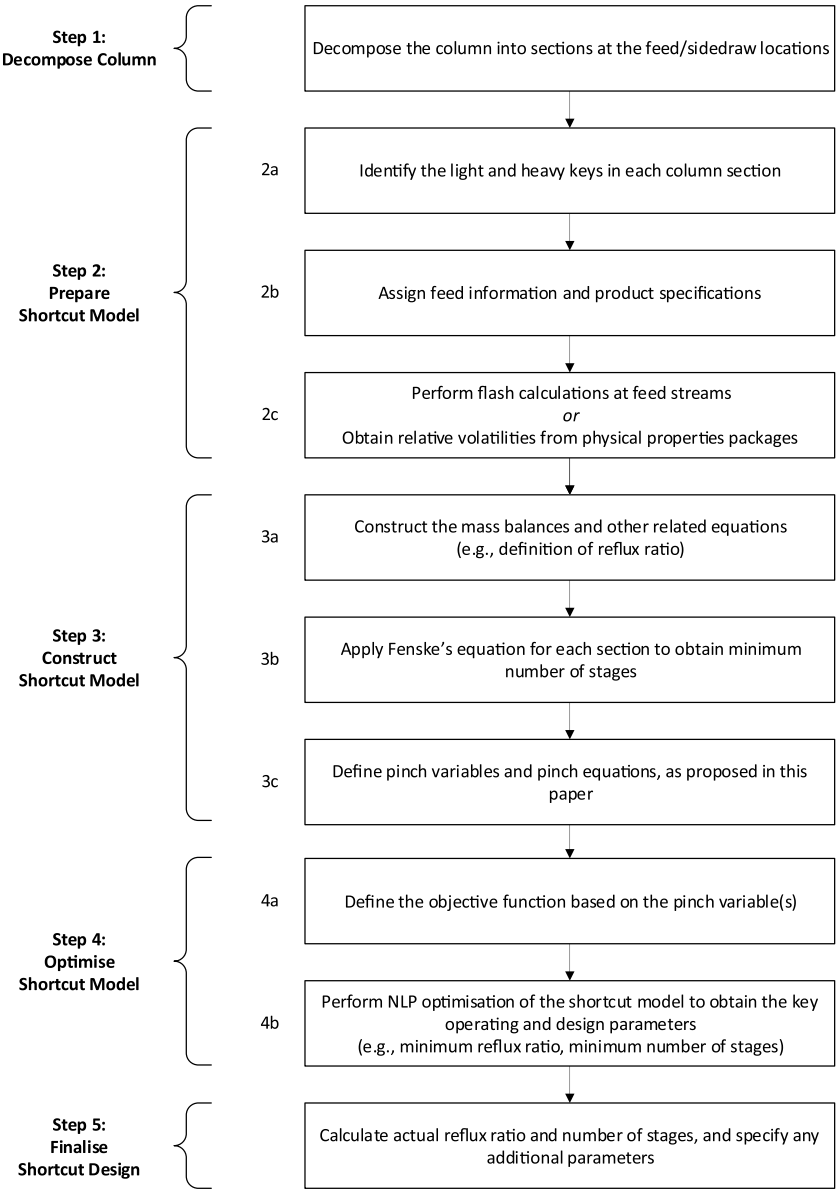

Fig. 1 – General flowchart of the shortcut calculation.

The shortcut method can be described in five major steps (see Fig. 1). First, the column is decomposed into different column sections at the feed/sidedraw locations. The columns sections used in this work, sections with or without reboiler and/or condenser, are shown in Fig. 2 (left) together with their corresponding shortcut structures (right). Then, the shortcut model is prepared by assigning all the known variables including the feed information and the main product specification in each product stream. After that, the shortcut model equations are constructed which includes the mass balances and Fenske's equation based on the shortcut structures in Fig. 2 (right). Also, additional variables and equations (e.g. the variables and equations describing the composition difference at each pinch point) are added to determine the quality of the pinch condition (detailed description below in step 3c). Next, the model is optimised, here using an NLP optimiser. The proposed objective function and initialisation method are described in detail below. Finally, the variables for the optimised shortcut design are transferred into the rigorous model and the rigorous simulation and/or optimisation is performed as normal.

To clearly illustrate the main concepts of the shortcut method, a detailed description for each step is given below using a single distillation column (shown in Fig. 2a) for a binary separation as an illustrative example, with calculation results for a specific system shown as Case study 1. The extension of the proposed shortcut method into more complex column designs is then presented for more complex configurations in Section 3.

2.1. *Step 1: Decompose the design into split column sections*

In the first step of the shortcut method (see Fig. 1), the conventional binary column is decomposed into different sections at the feed/sidedraw locations. Depending on the existence of a condenser and/or reboiler, the normal distillate and bottom streams may be replaced by an equation representing the net flow (F_d for the top section or F_b for the bottom section). The shortcut structure of the conventional column is shown in Fig. 2b. The structure allows for the feed to be split into vapour and/or liquid fractions. It should be noted that the proposed

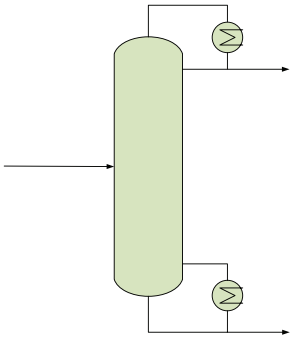

(a) Conventional distillation column

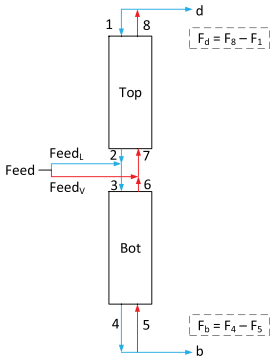

(b) Shortcut structure for Fig.2a

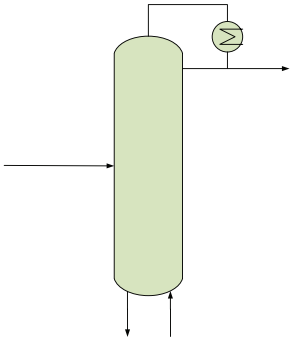

(c) Distillation column without a reboiler

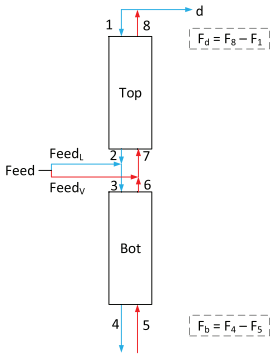

(d) Shortcut structure for Fig.2c

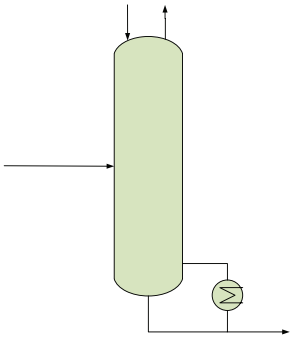

(e) Distillation column without a condenser

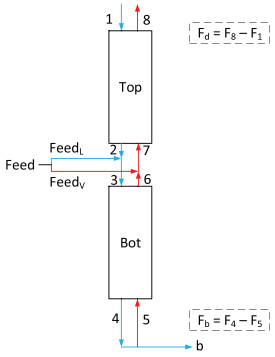

(f) Shortcut structure for Fig.2e

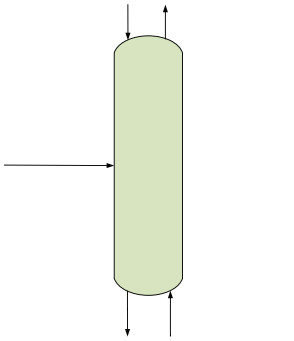

(g) Distillation column without a reboiler and condenser

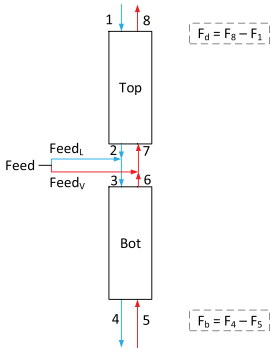

(h) Shortcut structure for Fig.2g

Fig. 2 – Schematics of the possible sectioning. Blue lines indicate liquid streams, red lines indicate vapour streams. The feed stream can also be a sidedraw stream if the flow direction is reversed. (For interpretation of the references to colour in this figure legend, the reader is referred to the web version of this article.).

shortcut method cannot handle a superheated and subcooled feed stream. However, a superheated stream can be estimated using the saturated vapour condition if the temperature difference is not significant, and similarly, a saturated liquid feed can be used for a subcooled feed stream.

2.2. Step 2: Prepare the shortcut model

Before starting the actual shortcut calculations, one has to identify the key components (step 2a) in each column sections based on the definition utilised by Fenske's equation. Also, the feed information including the feed flowrate, composition, pressure, and feed state (q) should be defined (step 2b). In addition, the product specifications (key component product composition or recovery) should be given, which is reasonable as the purity of the product is usually a known requirement. Next, a flash calculation (detailed equations in Appendix A) of the feed stream should be performed to obtain the relative volatility (step 2c) which in the following case studies is considered constant throughout the whole system at the feed condition as mentioned above. (If the relative volatility is provided, either as a value or as a function, it can be used directly instead.)

2.3. Step 3: Construct the shortcut model equations

In this step, the mass balances are first established (step 3a). The flowrate of each product stream (F_d for distillate and F_b for bottom stream) is considered to be equal to the amount of the corresponding main component in the feed stream for the example of a binary separation:

$$F_d = F_{feed} \times z_A \tag{1}$$

$$F_b = F_{feed} \times z_B \tag{2}$$

where A is the lighter component, and B is the heavier boiling component.

The reflux ratio is as usual defined as the liquid flow returned to the column over the distillate flow:

$$RR = \frac{F_1}{F_d} \tag{3}$$

Mass balance equations describing each stream are given by:

$$F_{feedL} = F_{feed} \times q \tag{4}$$

$$F_{feedV} = F_{feed} \times (1 - q) \tag{5}$$

$$F_2 = F_1 \tag{6}$$

$$F_3 = F_2 + F_{feedL} \tag{7}$$

$$F_4 = F_3 \tag{8}$$

$$F_5 = F_4 - F_b \tag{9}$$

$$F_6 = F_5 \tag{10}$$

$$F_7 = F_6 + F_{feedV} \tag{11}$$

$$F_8 = F_7 \tag{12}$$

The degree of freedom (DoF) for solving the mass balances is one, so the reflux ratio RR is selected to make the system well posed and is therefore the optimised decision variable in the shortcut method of the single distillation column.

According to the pinch condition, the compositions of each stream at the feed location ($x_{2,i}$, $x_{3,i}$, $y_{6,i}$, and $y_{7,i}$) are considered to be equal to the results from the flash calculation of the feed stream ($x_{feed,i}$ and $y_{feed,i}$):

$$x_{feed,i} = x_{2,i} = x_{3,i} \quad i \in \{A, B\} \tag{13}$$

$$y_{feed,i} = y_{6,i} = y_{7,i} \quad i \in \{A, B\} \tag{14}$$

At this stage, all the information required for applying the Fenske's equation in each section is known. Moving to step 3b, where Fenske's equation is defined as:

$$N_{min} = \frac{\ln\left[\left(\frac{x_{lk}}{x_{hk}}\right)_D / \left(\frac{x_{lk}}{x_{hk}}\right)_B\right]}{\ln(\alpha_{lk-hk})}$$

Taking the top section in the column as an example, the light key component is B and the heavy key component is A. The minimum number of stages required for both top and bottom sections, N_{min}^{top} and N_{min}^{bot}, are determined using the Fenske's equation, and will be rounded up to the nearest integer, as shown below

$$N_{min}^{top} = \left\lceil \frac{\ln\left[\left(\frac{x_{d,B}}{x_{d,A}}\right) / \left(\frac{x_{feed,B}}{x_{feed,A}}\right)\right]}{\ln(1/\alpha_{AB})} \right\rceil \tag{15}$$

$$N_{min}^{bot} = \left\lceil \frac{\ln\left[\left(\frac{x_{feed,B}}{x_{feed,A}}\right) / \left(\frac{x_{b,B}}{x_{b,A}}\right)\right]}{\ln(1/\alpha_{AB})} \right\rceil \tag{16}$$

These equations only introduce two new variables (N_{min}^{top} and N_{min}^{bot}) and no extra variable assignment is required. The total minimum number of stages of the column will be the summation of stages required for both sections and the feed location can be obtained directly, i.e. $N_{min} = N_{min}^{top} + N_{min}^{bot}$ and $N_{feed} = N_{min}^{top}$ when the stages are numbered from the top and down.

The shortcut model can now be solved by assigning just one variable (RR), but there is no guarantee that the pinch condition is achieved. Thus in step 3c, a pinch variable (Δ_{feed}) is introduced to reflect how close/far the condition is from the pinch condition. For the pinch condition of the feed location, the liquid and vapour compositions are already determined from the flash calculation of the feed stream. The component mass balances around the top column section can be established:

$$F_1 \times x_{1,i} + F_7 \times y_{feed,i}^{top} = F_2 \times x_{feed,i}^{top} + F_8 \times y_{8,i} \quad i \in \{A, B\} \tag{17}$$

where $x_{1,i}$ and $y_{8,i}$ can be assumed equal to the composition of the distillate, and $y_{feed,i}^{top}$ and $x_{feed,i}^{top}$ are the feed compositions calculated from mass balances around the top section of the column (i.e. not the same as $y_{feed,i}$ and $x_{feed,i}$ which are the compositions obtained through flash calculations).

By assigning either the value of $x_{feed,i}^{top}$ or $y_{feed,i}^{top}$, the value of the other composition can be calculated from the mass balance (Eq. (17)). For example, by providing the value of $x_{feed,i}^{top}$, Eq.

(17) can be rearranged to give the vapour composition entering the section:

$$y^{top}_{feed,i} = \frac{F_2 \times x^{top}_{feed,i} + F_8 \times y_{8,i} - F_1 \times x_{1,i}}{F_7} \quad i \in \{A, B\}$$

By applying the same method, the vapour composition at the feed location ($y^{bot}_{feed,i}$) can alternatively be obtained through the component mass balance around the bottom section.

The best design is achieved when, at the feed location, the composition changes are negligible for both liquid and vapour streams entering and leaving the stage. The approach to the pinch condition at the feed location (Δ_{feed}) can then be determined by calculating the difference between the vapour compositions calculated from the component balance ($y^{top}_{feed,A}$ and $y^{bot}_{feed,B}$) and the flash calculation of the dominant component in each section ($y_{feed,A}$ and $y_{feed,B}$) (this will be further explained in the case studies):

$$\begin{aligned} \Delta_{feed} &= \Delta_{feed,A} + \Delta_{feed,B} \\ \Delta_{feed} &= |y_{feed,A} - y^{top}_{feed,A}| + |y_{feed,B} - y^{bot}_{feed,B}| \end{aligned} \tag{18}$$

Note that for more complex systems, such as a dividing wall column, additional variables must be introduced to describe the features and constraints required, including the quality of the pinch condition at the thermal coupling locations (Δ_{tc}) and the potential requirement of the same number of stages across the wall (Δ_N). The detailed definitions of these variables will be presented later with the case studies.

2.4. *Step 4: Optimise the shortcut model*

As mentioned above, the optimal design is considered to be a design where there are no, or minimal, mixing effects at the feed location(s), in this work indicated by the pinch variable Δ_{feed} which should be as close to zero as possible. It can be shown that regardless of the mixture and feed composition, for an ideal binary system, the Δ_{feed} curve as a function of reflux ratio is always convex, so that a single point where Δ_{feed} is close to zero can be found. This point will indicate the point with the least mixing effects, and the corresponding reflux ratio can be treated as the minimum reflux ratio (RR_{min}) in the shortcut method. (As an example, Fig. 3 shows the relationship between reflux ratio and the pinch variable, Δ_{feed}, for different mixtures and different feed compositions.) Therefore, in order to obtain a shortcut design with the least mixing effect, i.e. minimum energy loss, the optimisation problem for a single distillation column to separate a binary mixture is defined as (step 4a):

$$\begin{aligned} \min_{RR} \quad & Z = \Delta_{feed} \\ \text{s.t.} \quad & RR \in [RR_{lb}, RR_{ub}] \end{aligned}$$

For other more complex systems involving more than one pinch variable, the optimisation problem is defined as

$$\begin{aligned} \min_{RR, R_{sl}, R_{sv}, \ldots} \quad & Z = \prod_{j \in S_{pv}} (\Delta_j + 1) \\ \text{s.t.} \quad & RR \in [RR_{lb}, RR_{ub}] \\ & R_{sl} \in [0, 1] \\ & R_{sv} \in [0, 1] \\ & \vdots \end{aligned}$$

where S_{pv} is the set of the pinch variables involved. It should be noted that the term "+1" is required to avoid the objective function Z becoming zero if any of the pinch variables are zero. For the ternary separation in the DWCs, it is also suggested to square the pinch stage variables relating the number of stages to increase its weighting, e.g. $(\Delta_N{}^2 + 1)$. Since the optimised variables are all continuous variables, a simple non-linear programming (NLP) solver is sufficient to solve the optimisation problem (step 4b).

2.5. *Step 5: Final shortcut design*

The optimisation of the shortcut design will identify the optimal minimum reflux ratio, RR_{min}, and the minimum number of stages in the column section, N_{min}. It should be noted that RR_{min} and N_{min} need to be scaled up to actual reflux ratio, RR, and actual number of stages, N, in rigorous simulations. Typical estimates for the actual reflux ratio and actual number of stages are (Sotudeh and Hashemi Shahraki, 2007; Dejanović et al., 2010a; Sorensen, 2014):

$$RR = 1.3 \times RR_{min} \tag{19}$$

$$N = 2 \times N_{min} \tag{20}$$

For other optimal variables considered for more complex systems, such as the flowrate of liquid or vapour sidedraw from the main column in a DWC, these should be kept as the values obtained from the shortcut optimisation when used for rigorous simulation.

3. Case studies

In the following, the proposed shortcut method presented in the previous section will be applied to four different case studies. The first case study is a simple conventional binary distillation column for which the equations in the shortcut method were outlined in the previous section. A novel shortcut method is perhaps not needed for such a simple system as other methods are already available, such as the classical FUGK method and the DSTWU (Winn-Underwood-Gilliland) model implemented in Aspen Plus (Aspen Technology Inc., 2017). Nevertheless, we will start by outlining our method for this system and compare with an existing method in a commercial simulator so as to illustrate the capabilities of our method. We will consider two different binary systems at different feed conditions as given in Table 1.

Next, to show the true power of the proposed shortcut method we will examine the performance of a dividing wall column (DWC, see Fig. 4a) and two reduced vapour transfer dividing wall columns (RVT-DWC), which are all extremely difficult to initialise in rigorous simulations. Agrawal (2000) proposed three RVT-DWC structures (see also Ramapriya et al. (2014) for the corresponding structures) for the separation of ternary mixtures as alternatives to the standard DWC, and the structures chosen as our case studies are the L-TC structure (see Fig. 5a) and the L-L structure (see Fig. 6a). (The TC-L structure is the inverse of the L-TC structure, thus only the L-TC structure is considered in this work.) Each of these RVT-DWCs are considered to be thermodynamically equivalent to a DWC when the reflux/boilup ratios on both sides of the RVT-DWC are equal to the reflux ratio of the DWC. The internal flowrates are obtained using the methods proposed by Ramapriya et al. (2014). Note that the reflux/boilup ratios on either side of the

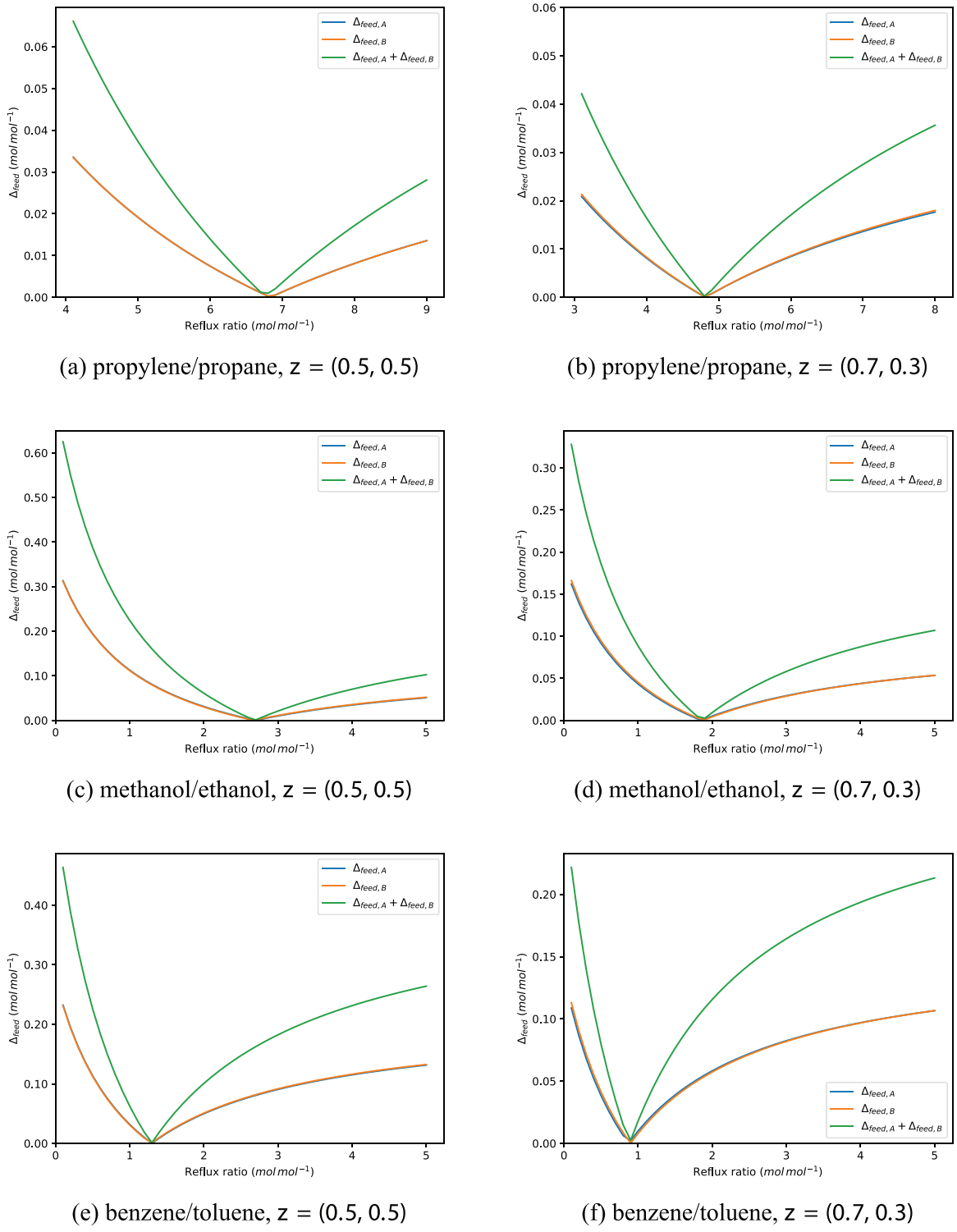

(a) propylene/propane, z = (0.5, 0.5)

(b) propylene/propane, z = (0.7, 0.3)

(c) methanol/ethanol, z = (0.5, 0.5)

(d) methanol/ethanol, z = (0.7, 0.3)

(e) benzene/toluene, z = (0.5, 0.5)

(f) benzene/toluene, z = (0.7, 0.3)

Fig. 3 – Relationship between the reflux ratio and feed composition pinch variable for different binary mixtures with different feed compositions z obtained from the shortcut model. Note that the blue and orange lines overlapped each other, and the design specifications are to achieve at least 0.99 mol mol^{-1} product in each product stream. (For interpretation of the references to colour in this figure legend, the reader is referred to the web version of this article.).

Table 1 – Feed information for the case study for binary separation (Case Study 1).

Item	Value	Unit
Mixtures	Propylene/propane, benzene/ethylbenzene	–
Feed compositions	(0.2, 0.8), (0.5, 0.5), (0.8, 0.2)	mol mol^{-1}
Feed/column pressure	1	bar
Feed condition	Saturated liquid	–
Feed flowrate	1000	kmol h^{-1}

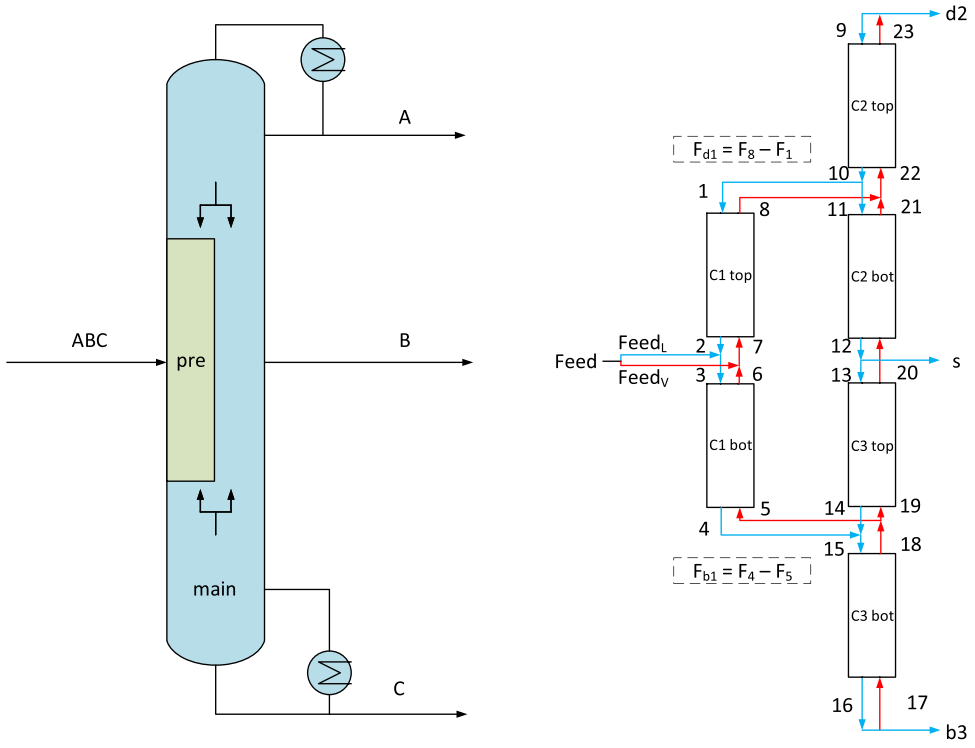

(a) Dividing wall column (b) Shortcut structure

Fig. 4 – Schematics of the dividing wall column. Blue lines indicate liquid streams, red lines indicate vapour streams. (For interpretation of the references to colour in this figure legend, the reader is referred to the web version of this article.).

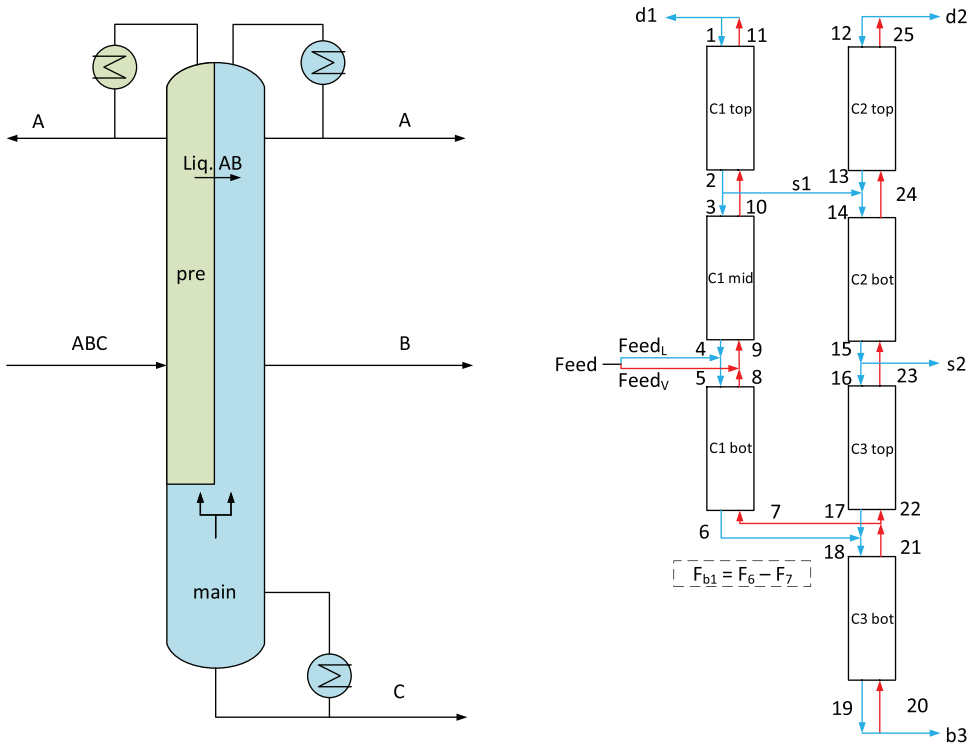

(a) L-TC Structure (b) Shortcut structure

Fig. 5 – Schematics of the L-TC structure. Blue lines indicate liquid streams, red lines indicate vapour streams. (For interpretation of the references to colour in this figure legend, the reader is referred to the web version of this article.).

wall can also be different. Our proposed shortcut method can handle both cases by adding or removing an equality equation between the reflux ratios on either side of the RVT-DWCs. To illustrate the use of the proposed shortcut method in these two situations, the reflux ratios in each section of the L-TC structure are considered to be the same (Case Study 3), while the reflux ratios and boilup ratios in each section of the L-L structure are considered to be different (Case Study 4). For DWC

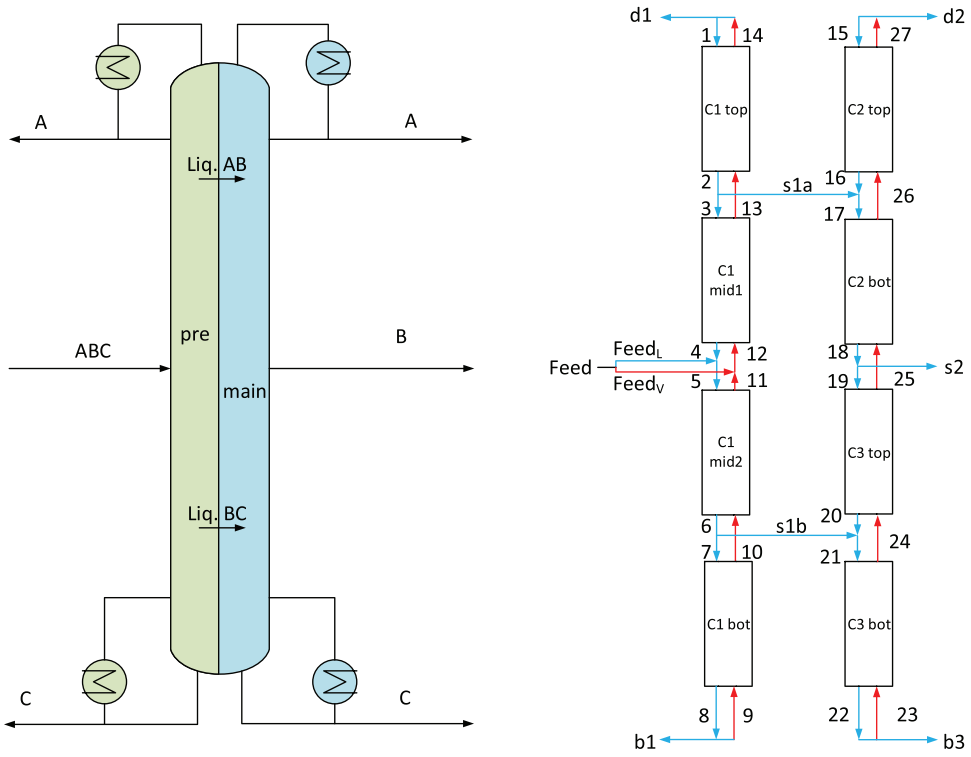

(a) L-L structure (b) Shortcut structure

Fig. 6 – Schematics of the L-L structure. Blue lines indicate liquid streams, red lines indicate vapour streams. (For interpretation of the references to colour in this figure legend, the reader is referred to the web version of this article.).

and RVT-DWCs considered in this work, the number of stages on both sides of the wall is assumed to be equal. This is considered as the special constraints, represented by Δ_N, which is part of the objective function (see details in the respective case studies). There may be cases where $\Delta_N \neq 0$ after optimisation in step 4. Thus, the column section (prefractionator or wall section in the main column) with lower number of stages should be scaled up to match the number of stages of the other column section while maintaining the ratio between the feed/sidedraw stage and stages of the corresponding column section. A discussion about Δ_N for these case studies can be found at the end of Section 3. For DWC, L-TC structure, and TC-L structure, where vapour transfer streams exist, the assumption/criteria of the same number of stages on both sides of the wall is valid when the pressure drop per stage on both sides of the wall is the same. However, for cases where the pressure drop per stage on both sides of the wall is considered to be different (i.e. the number of the stages on both sides of the wall is different), the special constraint will now be to achieve the same total pressure drop on both sides of the wall, represented by Δ_{PD}. To reflect the effects of the changing pressure on vapour-liquid equilibrium, relative volatility should not be considered as constant throughout the system. Instead, relative volatility models (e.g. flash calculations) should be applied for each pinch zone as part of the shortcut model in step 3, thus the relative volatility is simultaneously solved with the rest of the shortcut model in the optimisation (step 4).

In this work, the shortcut model equations are coded in gPROMS ModelBuilder and the optimisation step, step 4 in the shortcut method, is performed using the built-in NLP solver (SSOptTR), however, the method could of course just as easily have been coded using other tools as previously explained. To test the robustness of the shortcut designs presented in the case studies, the designs are transferred into commercial process simulators, such as gPROMS ProcessBuilder (Process Systems Enterprise, 2020) and Aspen Plus V10 (Aspen Technology Inc., 2017), for comparison with rigorous simulations. It should be noted that so far there are no library packages available for the DWC and RVT-DWCs designs in either simulator, thus the thermodynamically equivalent corresponding Petlyuk designs are used to represent the structures also for these rigorous simulations.

For all the case studies, when performing the shortcut method, the thermodynamic model in gPROMS is assumed to be the IDEAL model as this is the simplest model available. However, when performing rigorous simulations, the more accurate UNIQUAC model is used. While the UNIQUAC could also be used for the shortcut design, this would defeat the purpose of having as simple a calculation as possible. For the binary separations, propylene/propane ($\alpha = 1.29$) and benzene/ethylbenzene ($\alpha = 5.31$) are selected to examine the capability of handling both easy and difficult separations. For the ternary separations, two different mixtures are considered based on their ease of separation index (ESI) (Tedder and Rudd, 1978), where the ESI of benzene/toluene/o-xylene is less than one (0.87) and the ESI of n-butane/i-pentane/n-pentane is greater than one (2.02). Note that the ESI of each mixture is calculated at the equimolar condition. All the mixtures above are also considered for different feed compositions, and the feed information is shown in Table 1 for the binary mixtures and Table 2 for the ternary mixtures. For all the case studies, the product compositions in the respective product streams are specified to be $x_{spec,i} = 0.99\,\text{mol}\,\text{mol}^{-1}$.

Table 2 – Feed information for the case studies for ternary separation (Case Studies 2, 3, and 4).

Item	Value	Unit
Mixtures	Benzene/toluene/o-xylene, n-butane/i-pentane/n-pentane	–
Feed compositions	(0.10, 0.80, 0.10), (0.33, 0.34, 0.33), (0.60, 0.20, 0.20)	mol mol^{-1}
Feed/column pressure	1	bar
Feed condition	Saturated liquid	–
Feed flowrate	1000	kmol h^{-1}

3.1. *Case study 1: binary conventional column*

The structure of the binary conventional column is shown in Fig. 2a, and its shortcut structure is shown in Fig. 2b. The description for the shortcut method of a binary column was illustrated in the Methodology section. In this section, the column design (total number of stages, feed location and reflux ratio) obtained from the proposed shortcut method are compared with DSTWU shortcut method in Aspen Plus. The shortcut designs are simulated in the rigorous simulator, gPROMS ProcessBuilder, to obtain their corresponding product purities. Moreover, an optimised design is obtained from gPROMS ProcessBuilder using the built-in MINLP optimiser (OAERAP) for comparing the performance of both shortcut methods. For the optimisation of the rigorous model, the objective function is to minimise the total annualised cost (TAC, details of the cost equations can be found in Appendix C) subject to achieving at least 0.99 mol mol^{-1} product in each product stream. To ensure that the optimisation results are not affected by the initial guesses, the optimisation is repeated several times with different initial guesses. This is required as the optimisation algorithm does not guarantee global optimum. The shortcut and optimised results are shown in Table 3.

The results indicate that, in general, the shortcut method proposed in this work and DSTWU yield similar initial design and product purities. For the more difficult separation system (propylene/propane), the deviation in the estimate of the reflux ratio compared to DSTWU ranges from −0.4% to +4.4%, which shows a very good agreement, whilst the difference is larger for the easier separation system (benzene/ethylbenzene) but the absolute values are then quite small hence the larger error. The predicted number of stages from the proposed shortcut method is, however, up to 20% larger than for DSTWU. This is because DSTWU is using the Gilliland's and Kirkbride's equations to calculate the number of stages and feed locations, while Fenske's equation is used in this work. Comparing with the optimisation results from gPROMS ProcessBuilder, however, the proposed shortcut method shows a better agreement for the total number of stages. Moreover, both shortcut methods give reflux ratio close to the optimal results. Overall, there is a good agreement between the results from the proposed shortcut method and those from DSTWU for the two binary systems, showing that the proposed shortcut method is effective.

3.2. *Case study 2: dividing wall column*

Fig. 4a depicts a dividing wall column (DWC) used for ternary separations. The full corresponding DWC shortcut model can be found in Appendix B. In step 1 of the proposed shortcut method, the DWC is split into six sections based on the feed and sidedraw locations (see Fig. 4b), with the prefractionator represented by C1 and the main column represented by both C2 and C3. Component A is assumed to be the lightest component which is withdrawn at the top of the DWC, component B the middle component which exits through the side stream, and component C is the heaviest component withdrawn at the bottom (step 2a). The feed information can be found in Table 2 and the products are specified to be 0.99 mol mol^{-1} in their respective product stream (step 2b). Flash calculations are then performed (see Appendix A) to obtain the vapour and/or liquid composition of the mixture at the given feed condition (step 2c).

Similar to the binary design, in the shortcut method the flowrates of each product stream can be considered given by:

$$F_{d2} = F_{feed} \times z_A \tag{21}$$

$$F_s = F_{feed} \times z_B \tag{22}$$

$$F_{b3} = F_{feed} \times z_C \tag{23}$$

A few ratios are needed to describe the system. These are the standard reflux ratio (RR), the liquid split ratio (R_{sl}), and the vapour split ratio (R_{sv}):

$$RR = \frac{F_9}{F_{d2}} \tag{24}$$

$$R_{sl} = \frac{F_1}{F_{10}} \tag{25}$$

$$R_{sv} = \frac{F_5}{F_{18}} \tag{26}$$

The liquid and vapour splits are the main additional degrees of freedom for a DWC compared to a conventional column. The mass balances (step 3a) for the DWC can be established similarly to the ones described for the binary system. The degrees of freedom (DoF) required for solving the mass balances are three, so RR, R_{sl}, and R_{sv} are selected to make the system well posed, and these three variables are the optimised variables in the shortcut method.

There are three pinch zones in the DWC, one at the feed location and two at the top and bottom of the dividing wall. In the thermodynamically equivalent Petlyuk arrangement this becomes the feed location in the prefractionator (C1), and the thermal coupling locations with its connection with the main column (columns C2 and C3, respectively). It is assumed that all liquid streams entering and leaving a pinch zone have the same compositions, similarly for the vapour streams:

$$x_{feed,i} = x_{2,i} = x_{3,i} \quad i \in \{A, B, C\} \tag{27}$$

$$y_{feed,i} = y_{6,i} = y_{7,i} \quad i \in \{A, B, C\} \tag{28}$$

$$x_{tc1,i} = x_{1,i} = x_{10,i} = x_{11,i} \quad i \in \{A, B, C\} \tag{29}$$

$$y_{tc1,i} = y_{8,i} = y_{21,i} = y_{22,i} \quad i \in \{A, B, C\} \tag{30}$$

Table 3 – Case Study 1 – Single Conventional Column: Comparison between the results obtained for column design (N, N_{feed}, and RR) using proposed shortcut method and DSTWU (shortcut method built-in in Aspen Plus) for mixture A/B. The product compositions ($x_{d,A}$ and $x_{b,B}$) are obtained through rigorous simulations in gPROMS ProcessBuilder using the column design obtained from each shortcut method. The results are compared to optimal results obtained using a MINLP optimiser (OAERAP).

Variable	Propylene/propane			Benzene/ethylbenzene			Unit
Case	1.I	1.II	1.III	1.IV	1.V	1.VI	
z_A	0.20	0.50	0.80	0.20	0.50	0.80	mol mol^{-1}
z_B	0.80	0.50	0.20	0.80	0.50	0.20	mol mol^{-1}
Proposed Shortcut Method							
N	75	77	75	15	13	13	–
N_{feed}	49	39	27	9	7	5	–
RR	22.33	8.77	5.51	1.69	0.56	0.32	mol mol^{-1}
$x_{d,A}$	0.95	0.99	0.99	0.93	0.97	0.99	mol mol^{-1}
$x_{b,B}$	0.99	0.99	0.97	0.98	0.97	0.95	mol mol^{-1}
DSTWU Shortcut Method							
N	63	64	64	13	14	15	–
N_{feed}	32	33	33	7	8	8	–
RR	21.35	8.79	5.53	1.70	0.69	0.42	mol mol^{-1}
$x_{d,A}$	0.96	0.99	0.99	0.93	0.99	0.99	mol mol^{-1}
$x_{b,B}$	0.99	0.99	0.98	0.98	0.99	0.99	mol mol^{-1}
Optimisation							
N	86	82	84	20	19	15	–
N_{feed}	43	38	47	7	10	8	–
RR	20.88	8.36	4.73	1.81	0.55	0.22	mol mol^{-1}
$x_{d,A}$	0.99	0.99	0.99	0.99	0.99	0.99	mol mol^{-1}
$x_{b,B}$	0.99	0.99	0.99	0.99	0.99	0.99	mol mol^{-1}

$$x_{tc2,i} = x_{4,i} = x_{14,i} = x_{15,i} \quad i \in \{A, B, C\} \tag{31}$$

$$y_{tc2,i} = y_{5,i} = y_{18,i} = y_{19,i} \quad i \in \{A, B, C\} \tag{32}$$

where the subscripts $tc1$ refers to the top thermal coupling location (in $C2$, top of the wall), and $tc2$ refers to the bottom thermal coupling location (in $C3$, bottom of the wall) of the main column. The variables $x_{feed,i}$ and $y_{feed,i}$ had already been obtained from the flash calculations for the feed stream in step 2c.

To obtain the compositions of the thermal coupling streams, the component mass balances and constant relative volatility equations are required. A perfect separation between the key components in the prefractionator is assumed, i.e. only components A and B are present in the $C1$ *top* section, and only components B and C are present in the $C1$ *bot* section. Taking the top thermal coupling location as an example, and given that component A will only be present in $C1$ *top* and not in $C1$ *bot* (i.e. not in streams 3 or 6):

$$\alpha_{AB} = \frac{\alpha_{AC}}{\alpha_{BC}} = \frac{y_{tc1,A}/x_{tc1,A}}{y_{tc1,C}/x_{tc1,C}} \Big/ \frac{y_{tc1,B}/x_{tc1,B}}{y_{tc1,C}/x_{tc1,C}} = \frac{y_{tc1,A}/x_{tc1,A}}{y_{tc1,B}/x_{tc1,B}} \tag{33}$$

$$x_{tc1,C} = 0 \tag{34}$$

$$y_{tc1,C} = 0 \tag{35}$$

$$F_{feed} \times z_A = F_8 \times y_{tc1,A} - F_1 \times x_{tc1,A} \tag{36}$$

$$\sum_{i \in S_c} (y_{tc1,i}) = 1 \quad S_c = \{A, B, C\} \tag{37}$$

$$\sum_{i \in S_c} (x_{tc1,i}) = 1 \quad S_c = \{A, B, C\} \tag{38}$$

Eqs. (33)–(38) introduce six new variables ($x_{tc1,i}$ and $y_{tc1,i}$ for $i = \{A, B, C\}$) and six equations, therefore requiring no additional variable assignment. Similar equations are obtained for the bottom thermal coupling location, thus the compositions for all the thermal coupling streams can be determined.

The number of stages in each section can then be determined to find the total number of stages of each column, and their corresponding feed and sidedraw locations (step 3b). The only unknown information when applying Fenske's equation at this stage are the bottom liquid composition of $C2$, $x_{12,i}$, and the top liquid composition of $C3$, $x_{13,i}$. When calculating the number of stages, $C2$ and $C3$ are considered as two separated columns separating a binary mixture of AB and BC, respectively. Thus these liquid compositions (x_{12} and x_{13}) can be considered as:

$$x_{12} = (x_{12,A}, x_{12,B}, x_{12,C}) = (1 - x_{spec,B}, x_{spec,B}, 0) \tag{39}$$

$$x_{13} = (x_{13,A}, x_{13,B}, x_{13,C}) = (0, x_{spec,B}, 1 - x_{spec,B}) \tag{40}$$

Note that due to the assumption of perfect separation in the prefractionator, $x_{tc1,C} = 0$ and $x_{tc2,A} = 0$, the Fenske's equations involving these two variables are invalid. Therefore, specifically for the Fenske's equation, and for numerical reasons in solving the equation set, it is specified that $x_{tc1,C} = 1 \times 10^{-4}$ mol mol^{-1} and $x_{tc2,A} = 1 \times 10^{-4}$ mol mol^{-1}. It should also be kept in mind that if $x_{spec,B}$ is not high enough (e.g. $x_{spec,B} = 0.8$ mol mol^{-1}), there may be inconsistencies between x_{12} and x_{13}, leading to reduced performance of the proposed shortcut method.

The shortcut model can be solved as the DoF of the stage calculations is zero. The solution may, however, not yield an optimal solution or one that minimises the pinch condition. Therefore, in step 3c the pinch variables are introduced to find the pinch points around the feed location and the thermal coupling points, respectively:

$$\Delta_{feed} = |y_{feed,A} - y_{feed,A}^{C1,top}| + |y_{feed,C} - y_{feed,C}^{C1,bot}| \tag{41}$$

$$\Delta_{tc1} = |y_{tc1,A} - y_{tc1,A}^{C2,top}| \tag{42}$$

$$\Delta_{tc2} = |y_{tc2,C} - y_{tc2,C}^{C3,bot}| \tag{43}$$

$$\Delta_N = |(N^{C1,top} + N^{C1,bot}) - (N^{C2,bot} + N^{C3,top})| \tag{44}$$

where $y_{feed,A}^{C1,top}$, $y_{feed,C}^{C1,bot}$, $y_{tc1,A}^{C2,top}$, and $y_{tc2,C}^{C3,bot}$ can be calculated using mass balance equations similar to Eq. (17).

Note that Δ_{tc1} and Δ_{tc2} are described by the composition difference of only one component. This is because C2 and C3, where Δ_{tc1} and Δ_{tc2} are located, are considered to separate a binary mixture, and from Fig. 3 it can be seen that similar results can be obtained using the single component or the combined composition difference. Therefore, to simplify the equations, Δ_{tc1} and Δ_{tc2} are represented by the difference in only the dominant component. For Δ_{feed}, which is located in the prefractionator where a ternary mixture is present, the two dominant components, *A* (heavy key) and *C* (light key), are chosen to represent Δ_{feed}.

Moving to the optimisation step, step 4 of the proposed shortcut method, the optimisation problem is to minimise the product of the pinch variables by optimising the reflux ratio (RR), liquid split ratio (R_{sl}), and vapour split ratio (R_{sv}), and is mathematically described as:

$$\begin{aligned} \min_{RR,R_{sl},R_{sv}} \quad & Z = (\Delta_{feed} + 1) \times (\Delta_{tc1} + 1) \times (\Delta_{tc2} + 1) \times (\Delta_N{}^2 + 1) \\ \text{s.t.} \quad & RR \in [RR_{lb}, RR_{ub}] \\ & R_{sl} \in [0, 1] \\ & R_{sv} \in [0, 1] \end{aligned}$$

Note that Δ_N is squared to increase its weighting in the objective function as it is the main design constraint for the DWC.

The results are shown in Table 4 for the two chemical systems at three different feed compositions: rich in the intermediate component, equimolar, and somewhat rich in the light component. Note that the liquid and vapour split ratios (R_{sl} and R_{sv}) are not used directly in the rigorous simulation, instead they are converted into sidedraw flowrates (F_{sl} and F_{sv}) through:

$$F_{sl} = F_1 = F_{10} \times R_{sl} \tag{45}$$

$$F_{sv} = F_5 = F_{18} \times R_{sv} \tag{46}$$

The flowrates and compositions of the thermal coupling streams obtained from the shortcut method and the final shortcut design values are also shown in Table 4, where the actual reflux ratio and number of stages have been obtained by Eqs. (19) and (20), respectively. These results are essential for the initialisation of an rigorous model, and having these shortcut values will significantly reduce the time and failure rate of convergence. Note that there are currently no commercial packages available that have models for even standard DWCs, let alone shortcut methods for their design, hence our results cannot be compared, just discussed. We will, however, compare with our own optimal results later.

The results indicate that for the benzene/toluene/o-xylene mixture, which has moderate relative volatility between each pair of adjacent components, the proposed shortcut method can provide a good initial design where the product purity is close to the product specification (largest deviation is 0.05 mol mol^{-1}), regardless of the feed composition. For the n-butane/i-pentane/n-pentane mixture, the relative volatility between i-pentane and n-pentane is small (1.36), making their separation difficult. The deviation between the product purity obtained from the proposed shortcut method and the product specification is larger compared to the benzene/toluene/o-xylene mixture, especially when the feed composition of i-pentane and/or n-pentane is small. These initial designs nevertheless provide a good feasible simulation with at least one of the product composition close to the specification, largest deviation is 0.1 mol mol^{-1}, and will therefore provide a good starting point for a rigorous simulation.

3.3. *Case study 3: reduced vapour transfer dividing wall column: L-TC structure*

The L-TC structure is a reduced vapour transfer DWC (RVT-DWC), initially introduced by Agrawal (2000), which is a modification of a DWC and also intended for separating ternary mixtures. The top vapour thermal coupling stream is removed and the configuration has a single liquid stream going from the prefractionator side to the main column side, as shown in Fig. 5a, hence the term L-TC structure since the top thermal coupling streams (TC) in the regular DWC are substituted with a single liquid stream (L). The thermal coupling streams (TC) are still present at the bottom of the wall as for a normal DWC. The upper section of the dividing wall is extended all the way up to the top of the column, resulting in two condensers and two distillate streams, thus two reflux ratios are needed. The reflux ratios on both sides of the L-TC structure can be different, but in this case study they are considered to be the same (but in the next case study they are different).

In step 1, the L-TC structure consists of seven sections, as shown in Fig. 5b. In the top section of the prefractionator (*C1 top*), the key components are *A* (heavy key) and *B* (light key) as no *C* is assumed to be present in both the inlet and outlet streams of *C1 top*.

The equations used to build the shortcut model (step 3a) of the L-TC configurations are similar to those used in a DWC (see Appendix B), therefore only the differences are considered here. As there are two product streams for the light component A, Eq. (21) is invalid, so another set of relationships should be defined:

$$F_{d1} + F_{d2} = F_{feed} \times z_A \tag{47}$$

$$R_d = \frac{F_{d2}}{F_{feed} \times z_A} \tag{48}$$

where R_d is the distribution ratio of the main column distillate.

The definitions for the reflux ratios and vapour split ratios are similar to those of the DWC. However, in the L-TC structure, the liquid transfer stream (stream s1) is now extracted from the prefractionator to the main column instead of the other way around as for the DWC, so the liquid split ratio is redefined as:

$$R_{sl} = \frac{F_{s1}}{F_2} \tag{49}$$

Also, since the reflux ratios on either sides of the L-TC structure are considered the same in this case study:

$$RR^{pre} = RR^{main} \tag{50}$$

After constructing the mass balances of the L-TC structure similarly to the DWC, the DoF so far is three. It is suggested to choose RR^{main}, R_{sl} and either one from R_{sv} and R_d (as choos-

Table 4 – Case Study 2 – Dividing Wall Column: Input parameters (obtained from the proposed shortcut method) and final product composition (obtained from gPROMS ProcessBuilder) for feed mixture of A/B/C at different feed composition z. The thermal coupling stream information (obtained from the proposed shortcut method) can be used as initial values in rigorous simulation.

Variable	Benzene/toluene/o-xylene			n-Butane/i-pentane/n-pentane			Unit
Case	2.I	2.II	2.III	2.IV	2.V	2.VI	
z_A	0.10	0.33	0.60	0.10	0.33	0.60	mol mol^{-1}
z_B	0.80	0.34	0.20	0.80	0.34	0.20	mol mol^{-1}
z_C	0.10	0.33	0.20	0.10	0.33	0.20	mol mol^{-1}
Prefractionator							
N^{pre}	16	22	20	24	32	38	–
N^{pre}_{feed}	8	12	8	12	14	18	–
Main Column							
N^{main}	47	45	43	85	81	79	–
$N^{C2}_{feed}/N^{C3}_{feed}$	17/34	13/36	11/32	15/40	15/48	9/48	–
N_s	27	25	23	21	21	21	–
N_{sl}/N_{sv}	17/34	13/36	11/32	15/40	15/48	9/48	–
F_{sl}	172.41	118.67	130.51	387.24	1057.56	220.91	kmol h^{-1}
F_{sv}	499.93	578.40	805.69	593.52	1398.82	879.42	kmol h^{-1}
F_s	800	340	200	800	340	200	kmol h^{-1}
RR^{main}	17.03	2.52	1.14	38.64	11.01	2.51	mol mol^{-1}
F_{d2}	100	330	600	100	330	600	kmol h^{-1}
Product Purity							
$x_{d2,A}$	0.95	0.99	0.99	0.99	0.99	0.99	mol mol^{-1}
$x_{s,B}$	0.99	0.94	0.96	0.98	0.98	0.90	mol mol^{-1}
$x_{b3,C}$	0.97	0.95	0.97	0.89	0.98	0.91	mol mol^{-1}
Thermal Coupling Streams Information							
Stream *sl*							
F_{sl}	172.41	118.67	130.51	387.24	1057.56	220.91	kmol h^{-1}
$x_{sl,A}$	0.1181	0.4495	0.7106	0.1039	0.1743	0.6613	mol mol^{-1}
$x_{sl,B}$	0.8819	0.5505	0.2894	0.8961	0.8257	0.3387	mol mol^{-1}
$x_{sl,C}$	0	0	0	0	0	0	mol mol^{-1}
Stream 8							
F_8	499.93	578.40	805.69	593.52	1398.82	879.42	kmol h^{-1}
$y_{8,A}$	0.2408	0.6627	0.8598	0.2363	0.3677	0.8484	mol mol^{-1}
$y_{8,B}$	0.7592	0.3373	0.1402	0.7637	0.6232	0.1516	mol mol^{-1}
$y_{8,C}$	0	0	0	0	0	0	mol mol^{-1}
Stream 4							
F_4	1172.41	1118.67	1130.51	1387.24	2057.56	1220.91	kmol h^{-1}
$x_{4,A}$	0	0	0	0	0	0	mol mol^{-1}
$x_{4,B}$	0.8974	0.6064	0.7490	0.8928	0.6423	0.6064	mol mol^{-1}
$x_{4,C}$	0.1026	0.3936	0.2510	0.1072	0.3577	0.3936	mol mol^{-1}
Stream *sv*							
F_{sv}	499.93	578.40	805.69	593.52	1398.82	879.42	kmol h^{-1}
$y_{sv,A}$	0	0	0	0	0	0	mol mol^{-1}
$y_{sv,B}$	0.9593	0.8094	0.8961	0.9179	0.7098	0.6810	mol mol^{-1}
$y_{sv,C}$	0.0407	0.1906	0.1039	0.0821	0.2902	0.3190	mol mol^{-1}

ing both R_{sv} and R_d will result in a high-index problem). In this case study, R_{sv} is chosen as the assigned and optimised variable together with RR^{main} and R_{sl}. Next, the composition equality equations at the pinch zones (similar to Eqs. (27) and (32)), and the equations used to obtain the compositions of the thermal couplings streams and the liquid transfer stream from the prefractionator (similar to Eqs. (33) and (38)) should be developed.

Then, in step 3b, similar to the case of the DWC, Fenske's equation is applied in each section to find the number of stages. So far, no extra DoFs are introduced in the system. Similar to the DWC, the pinch variables are defined (step 3c) as:

$$\Delta_{feed} = |y_{feed,A} - y^{C1,mid}_{feed,A}| + |y_{feed,C} - y^{C1,bot}_{feed,C}| \quad (51)$$

$$\Delta^{pre}_{sl} = |y_{sl,A} - y^{C1,top}_{sl,A}| \quad (52)$$

$$\Delta^{main}_{sl} = |y_{sl,A} - y^{C2,top}_{sl,A}| \quad (53)$$

$$\Delta_{tc} = |y_{tc,C} - y^{C3,bot}_{tc,C}| \quad (54)$$

$$\Delta_N = |(N^{C1,mid} + N^{C1,bot}) - (N^{C2,bot} + N^{C3,top})| \quad (55)$$

It should be noted that the liquid transfer stream (F_{s1}) brings about two pinch zones, one pinch zone in each of the prefractionator and the main column, thus two pinch variables (Δ^{pre}_{sl} and Δ^{main}_{sl}) are defined for this location. Also, when defining the stage difference between each side of the wall, the top section of each column ($N^{C1,top}$ and $N^{C2,top}$) are ignored as, according to Fenske's equation, they will have the same number of stages due to the same compositions and key components involved. It should be noted that, practically, the liquid sidedraw stream from the prefractionator can be sent into a different stage in the main column. In the rigorous simulations, the actual sidedraw/feed stage of the liquid sidedraw stream should be obtained from a MINLP optimiser.

Moving to the optimisation step (step 4), the optimisation problem is to minimise the product of the pinch variables

Table 5 – Case Study 3 – L-TC Structure: Input parameters (obtained from the proposed shortcut method) and final product composition (obtained from gPROMS ProcessBuilder) for feed mixture of A/B/C at different feed composition z. The thermal coupling and liquid transfer stream information (obtained from the proposed shortcut method) can be used as initial values in rigorous simulation.

Variable	Benzene/toluene/o-xylene			n-Butane/i-pentane/n-pentane			Unit
Case	3.I	3.II	3.III	3.IV	3.V	3.VI	
z_A	0.10	0.33	0.60	0.10	0.33	0.60	mol mol^{-1}
z_B	0.80	0.34	0.20	0.80	0.34	0.20	mol mol^{-1}
z_C	0.10	0.33	0.20	0.10	0.33	0.20	mol mol^{-1}
Prefractionator							
N^{pre}	33	31	31	39	51	47	–
N^{pre}_{feed}	25	21	19	27	29	25	–
N_{s1}	17	9	9	17	7	7	–
F_{s1}	426.34	202.02	235.77	520.35	230.07	359.55	kmol h^{-1}
RR^{pre}	15.28	3.28	2.15	32.22	7.25	3.09	mol mol^{-1}
Main Column							
N^{main}	47	43	43	85	83	79	–
$N^{C2}_{feed}/N^{C3}_{feed}$	17/34	9/32	9/32	17/40	7/52	7/48	–
N_{s2}	25	23	23	21	23	21	–
N_{sv}	34	32	32	40	52	48	–
F_{sv}	674.59	580.42	1136.58	1804.71	779.75	1005.73	kmol h^{-1}
F_s	800	340	200	800	340	200	kmol h^{-1}
RR^{main}	15.28	3.28	2.15	32.22	7.25	3.09	mol mol^{-1}
F_{d2}	47.10	165.12	171.21	30.00	211.40	302.06	kmol h^{-1}
Product Purity							
$x_{d1,A}/x_{d2,A}$	0.99/0.98	0.99/0.93	0.99/0.99	0.99/0.98	0.99/0.99	0.99/0.99	mol mol^{-1}
$x_{s2,B}$	0.99	0.96	0.99	0.97	0.91	0.98	mol mol^{-1}
$x_{b3,C}$	0.95	0.99	0.99	0.79	0.91	0.99	mol mol^{-1}
Thermal Coupling and Liquid Transfer Streams Information							
Stream s1							
F_{s1}	426.34	202.02	235.77	520.35	230.07	359.55	kmol h^{-1}
$x_{s1,A}$	0.1117	0.8255	0.7444	0.0590	0.9240	0.8484	mol mol^{-1}
$x_{s1,B}$	0.8883	0.1745	0.2556	0.9410	0.0760	0.1516	mol mol^{-1}
$x_{s1,C}$	0	0	0	0	0	0	mol mol^{-1}
Stream 6							
F_6	1195.35	1213.32	1472.02	2214.37	1431.08	1348.24	kmol h^{-1}
$x_{6,A}$	0	0	0	0	0	0	mol mol^{-1}
$x_{6,B}$	0.8921	0.6498	0.8041	0.8792	0.5805	0.6288	mol mol^{-1}
$x_{6,C}$	0.1079	0.3502	0.1959	0.1208	0.4195	0.3712	mol mol^{-1}
Stream sv							
F_{sv}	674.59	580.42	1136.58	1804.71	779.75	1005.73	kmol h^{-1}
$y_{sv,A}$	0	0	0	0	0	0	mol mol^{-1}
$y_{sv,B}$	0.9571	0.8364	0.9222	0.9072	0.6534	0.7012	mol mol^{-1}
$y_{sv,C}$	0.0429	0.1636	0.0778	0.0928	0.3466	0.2988	mol mol^{-1}

by optimising the reflux ratio (RR), liquid split ratio (R_{sl}), and vapour split ratio (R_{sv}), and is mathematically described as:

$$\min_{RR^{main},R_{sl},R_{sv}} \quad Z = (\Delta_{feed}+1)\times(\Delta_{sl}^{pre}+1)\times(\Delta_{sl}^{main}+1)\times(\Delta_{tc}+1)\times(\Delta_N{}^2+1)$$

$$\text{s.t.} \quad RR^{main} \in [RR^{main}_{lb}, RR^{main}_{ub}]$$

$$R_{sl} \in [0,1]$$

$$R_{sv} \in [0,1]$$

The results are tabulated in Table 5, and conclusions similar to the conclusions for the DWC in Section 3.2 can be made. The results show good agreement with the product specifications for each product stream for the benzene/toluene/o-xylene mixture. For the n-butane/i-pentane/n-pentane mixture, with close relative volatility between i-pentane and n-pentane, the greatest difference in the product specification is 0.2 mol mol^{-1} for n-pentane when the feed composition is (0.10, 0.80, 0.10) (Case 3.IV). This is due both to the difficult separation and the small amount of n-pentane in the feed.

3.4. *Case study 4: reduced vapour transfer dividing wall column: L-L structure*

Fig. 6a depicts a type of RVT-DWC called the L-L structure, also initially proposed by Agrawal (2000) for separation of ternary mixtures. It gets its name as both the streams in the top and bottom thermal coupling sections are replaced by single liquid streams. The column is divided entirely from the top to the bottom by the dividing wall, thus the configuration has two condensers, two reboilers, two reflux ratios, and two boilup ratios, one of each on either side of the dividing wall. The reflux/boilup ratios on either side of the L-L structure can be the same as for Case study 3, but in this case study, they are considered to be different.

As shown in Fig. 6b, there are eight sections in the L-L structure (step 1). Compared to a standard DWC, two extra sections, *C1 top* and *C1 bot*, are used to achieve the separation task between the binary mixtures *AB* and *BC*, respectively. In step 3a, the mass balances are constructed. Similar to the L-TC structure, the shortcut model of the L-L structure contains reflux ratios in the prefractionator (RR^{pre}) and the main column (RR^{main}), the distribution ratio of the main column distillate

Table 6 – Case Study 4 – L-L Structure: Input parameters (obtained from the proposed shortcut method) and final product composition (obtained from gPROMS ProcessBuilder) for feed mixture of A/B/C at different feed composition z. The liquid transfer stream information (obtained from the proposed shortcut method) can be used as initial values in rigorous simulation.

Variable	Benzene/toluene/o-xylene			n-Butane/i-pentane/n-pentane			Unit
Case	4.I	4.II	4.III	4.IV	4.V	4.VI	
z_A	0.10	0.33	0.60	0.10	0.33	0.60	mol mol^{-1}
z_B	0.80	0.34	0.20	0.80	0.34	0.20	mol mol^{-1}
z_C	0.10	0.33	0.20	0.10	0.33	0.20	mol mol^{-1}
Prefractionator							
N^{pre}	47	47	43	85	83	81	–
N^{pre}_{feed}	25	25	17	27	27	27	–
N_{sl1a}/N_{sl1b}	17/33	13/35	5/31	17/39	7/49	9/49	–
F_{sl1a}	540.89	293.81	309.51	718.44	181.33	328.39	kmol h^{-1}
F_{sl1b}	353.17	280.52	242.96	123.22	495.05	193.73	kmol h^{-1}
RR^{pre}	21.95	2.99	2.23	32.15	5.78	2.02	mol mol^{-1}
F_{d1}	42.19	199.95	301.39	72.95	164.10	356.51	kmol h^{-1}
Main Column							
N^{main}	47	47	43	85	83	81	–
$N^{C2}_{feed}/N^{C3}_{feed}$	17/33	13/35	5/31	17/39	7/49	9/49	–
N_{s2}	25	25	23	21	23	21	–
F_{s2}	800	340	200	800	340	200	kmol h^{-1}
RR^{main}	8.80	1.99	2.29	19.47	8.35	1.90	mol mol^{-1}
F_{d2}	57.81	130.05	298.61	27.05	165.90	243.49	kmol h^{-1}
Product Purity							
$x_{d1,A}/x_{d2,A}$	0.99/0.93	0.99/0.99	0.99/0.99	0.99/0.83	0.99/0.99	0.99/0.99	mol mol^{-1}
$x_{s2,B}$	0.99	0.98	0.98	0.96	0.88	0.89	mol mol^{-1}
$x_{b1,C}/x_{b3,C}$	0.94/0.93	0.98/0.98	0.99/0.99	0.71/0.85	0.82/0.93	0.89/0.88	mol mol^{-1}
Liquid Transfer Streams Information							
Stream *s1a*							
F_{s1a}	540.89	293.81	309.51	718.44	181.33	328.39	kmol h^{-1}
$x_{s1a,A}$	0.1077	0.4495	0.9745	0.0387	0.9240	0.7523	mol mol^{-1}
$x_{s1a,B}$	0.8923	0.5505	0.0255	0.9613	0.0760	0.2477	mol mol^{-1}
$x_{s1a,C}$	0	0	0	0	0	0	mol mol^{-1}
Stream *s1b*							
F_{s1b}	353.17	280.52	242.96	123.22	495.05	193.73	kmol h^{-1}
$x_{s1b,A}$	0	0	0	0	0	0	mol mol^{-1}
$x_{s1b,B}$	0.8955	0.6202	0.7723	0.8745	0.6524	0.5878	mol mol^{-1}
$x_{s1b,C}$	0.1045	0.3798	0.2277	0.1255	0.3476	0.4122	mol mol^{-1}

(R_d), and two liquid split ratios in the prefractionator (R_{sl1a} and R_{sl1b}). Considering only the mass balances of the L-L model, the DoF is five. Thus, all the ratio variables (RR^{pre}, RR^{main}, R_d, R_{sl1a}, and RR_{sl1b}) must be specified to make the model well posed.

After applying the Fenske's equation (step 3b), the pinch variables are defined (step 3c) as:

$$\Delta_{feed} = |y_{feed,A} - y^{C1,mid1}_{feed,A}| + |y_{feed,C} - y^{C1,mid2}_{feed,C}| \quad (56)$$

$$\Delta^{pre}_{sl1a} = |y_{sl1a,A} - y^{C1,top}_{sl1a,A}| \quad (57)$$

$$\Delta^{main}_{sl1a} = |y_{sl1a,A} - y^{C2,top}_{sl1a,A}| \quad (58)$$

$$\Delta^{pre}_{sl1b} = |y_{sl1b,C} - y^{C1,bot}_{tc1b,C}| \quad (59)$$

$$\Delta^{main}_{sl1b} = |y_{sl1b,C} - y^{C3,bot}_{tc1b,C}| \quad (60)$$

$$\Delta_N = |(N^{C1,mid1} + N^{C1,mid2}) - (N^{C2,bot} + N^{C3,top})| \quad (61)$$

The optimisation problem can be written as:

$$\min_{RR^{pre},RR^{main},R_d,R_{sl1a},R_{sl1b}} \quad Z = (\Delta_{feed}+1) \times (\Delta^{pre}_{sl1a}+1) \times (\Delta^{main}_{sl1a}+1) \times (\Delta^{pre}_{sl1b}+1) \times (\Delta^{main}_{sl1b}+1) \times (\Delta_N{}^2+1)$$

$$\text{s.t.} \quad RR^{pre} \in [RR^{pre}_{lb}, RR^{pre}_{ub}]$$

$$RR^{main} \in [RR^{main}_{lb}, RR^{main}_{ub}]$$

$$R_d \in [0,1]$$

$$R_{sl1a} \in [0,1]$$

$$R_{sl1b} \in [0,1]$$

The designs obtained from the proposed shortcut method are presented in Table 6. For the benzene/toluene/o-xylene mixture, the proposed shortcut method yields shortcut designs whose purities are very close to the product specification, with a maximum deviation of 0.06 mol mol^{-1} from the 0.99 mol mol^{-1} product specification at the extreme molar feed compositions of (0.1, 0.8, 0.1) (Case 4.I). The shortcut design for the n-butane/i-pentane/n-pentane mixture is also fairly good although the prediction for n-pentane (maximum 0.28 mol mol^{-1} difference in Case 4.IV) is far from the specification.

In all the case studies for ternary separations, it is found that at a specific mixture and feed composition, Δ_N does

Table 7 – Comparison between results obtained from proposed shortcut method (SC) and results after optimising with GA-OAERAP (OPT), using Case Study 2 - Dividing Wall Column for separation of benzene/toluene/o-xylene mixture at different feed composition z.

Variable	SC	OPT	SC	OPT	SC	OPT	Unit
z_{bezene}	0.10		0.33		0.60		mol mol^{-1}
$z_{toluene}$	0.80		0.34		0.20		mol mol^{-1}
z_{xylene}	0.10		0.33		0.20		mol mol^{-1}
Prefractionator							
N^{pre}	16	20	22	26	20	21	–
N^{pre}_{feed}	8	12	12	12	8	8	–
Main Column							
N^{main}	47	45	45	49	43	41	–
$N^{C2}_{feed}/N^{C3}_{feed}$	17/34	12/33	13/36	9/36	11/32	9/31	–
N_s	27	23	25	21	23	22	–
F_{sl}	172.41	245.13	118.67	221.56	130.51	217.84	kmol h^{-1}
F_{sv}	499.93	744.85	578.40	676.10	805.69	843.90	kmol h^{-1}
F_s	800	806.12	340	336.77	200	193.88	kmol h^{-1}
RR^{main}	17.03	13.87	2.52	2.58	1.14	1.04	mol mol^{-1}
F_{d2}	100	99.75	330	332.88	600	605.32	kmol h^{-1}
Product Purity							
$x_{d2,benzene}$	0.95	0.99	0.99	0.99	0.99	0.99	mol mol^{-1}
$x_{s,toluene}$	0.99	0.99	0.94	0.99	0.96	0.99	mol mol^{-1}
$x_{b3,xylene}$	0.97	0.99	0.95	0.99	0.97	0.99	mol mol^{-1}
TAC	8.84	7.31	6.05	6.28	6.55	6.31	M$ y^{-1}
CPU time*	–	1468	–	3339	–	1957	s

* GA-OAERAP is performed on a desktop (AMD Ryzen 9 3900X CPU, 3.79 GHz, 64 GB memory). GA is performed in MATLAB with the parallel computing function (18 workers).

not vary much with the DWC designs (e.g. Δ_N is 1 for equi-molar benzene/toluene/o-xylene in DWC, L-TC structure, and L-L structure). This is expected as these DWC designs have similar separation principles, thus similar separation performances. Besides, the Δ_N is relatively smaller for the benzene/toluene/o-xylene mixture (e.g. largest Δ_N is 3 and 8 for benzene/toluene/o-xylene and n-butane/i-pentane/n-pentane, respectively). Based on the results from each case study, it can be found that with smaller Δ_N (for benzene/toluene/o-xylene mixture), the product purity obtained from the rigorous simulations is closer to the design specifications. It can also be seen that the prediction of the product purity at extreme feed compositions have deviations from the specified product purity, especially for the mixture with adjacent components with low relative volatility. Nevertheless, the proposed shortcut method still provides a very good initialisation for the rigorous simulations even at extreme feed conditions, as will be shown next.

4. Comparison between shortcut and optimal designs

To reflect on how close the results from the shortcut method are to an optimal design, the results from the most commonly used dividing wall column (DWC) are compared to their corresponding optimised designs for the benzene/toluene/o-xylene mixture (i.e. Case study 2 with the first mixture).

As the DWC is complex and highly integrated, there are convergence issues not only for the optimisation but also for the simulation. Thus, the combined stochastic-deterministic (GA-OAERAP) optimisation approach proposed in our previous work (Chia et al., 2021) is utilised to address the convergence problem. In the combined optimisation approach, a stochastic method is combined with a deterministic method. In this work, a preliminary genetic algorithm (GA) with a looser fitness tolerance is used to find an approximate, preliminary, optimal design which is then used as initial values in the final deterministic MINLP optimiser, which is an Outer Approximation/Equality Relaxation/Augmented Penalty (OAERAP). All optimisations were performed using a desktop with an AMD Ryzen 9 3900X CPU with 3.79 GHz and 64 GB memory. Moreover, the parallel computing (18 workers) function in MATLAB was activated to speed up the GA process.

The preliminary GA is user-defined in MATLAB (The MathWorks Inc, 2019) and the process simulations are performed in gPROMS ProcessBuilder (Process Systems Enterprise, 2020), with the data transfer handled by gO:MATLAB (Process Systems Enterprise, 2019). The preliminary optimal design obtained from the GA optimisation is used to initialise the OAERAP built-in in gPROMS ProcessBuilder. The details and settings of both the preliminary GA and OAERAP can be found in Chia et al. (2021). The objective function considered is the total annualised cost (TAC) of the DWC, which includes the capital costs (for the column shell, column internals, reboiler, and condenser) and operating cost (for only the reboiler utility), as detailed in Tsatse et al. (2021). While performing the simulation, due to the lack of commercial packages for DWC, a Petlyuk design is used as also considered in most of the open literature. Thus, when calculating the DWC column dimensions (needed for capital costs calculations), the total area needed in the DWC is considered to be equal to the sum of the areas obtained for the two columns in the Petlyuk design (prefractionator and main column). The dimension and cost equations considered can be found in Appendix C.

The results (design and operating variables, product purity, and TAC) from both the shortcut method and the optimisation are presented in Table 7. The results show that the shortcut design is very close to the optimal design. The number of stages in the main column is only 2 or 4 stages different from the optimal number of stages, and the shortcut method may either over- or under-predict the optimal number. The number of stages in the prefractionator is also fairly close, as are the feed and sidedraw locations. The reflux ratios were of

the same order of magnitude for all the three feed conditions considered, e.g. 17.03 compared to 13.87 for the mixture rich in component B and 2.52 compared with 2.58 for the equimolar mixture. It can be seen that the flow rates of the thermal transfer streams are quite different, e.g. 499.93 kmol h^{-1} for the vapour transfer stream F_{sv} from the shortcut method compared to 744.85 kmol h^{-1} for the optimal solution, but having the initial values for these streams greatly improve the optimisation initialisation and convergence. Note that the optimisation has been repeated for a number of different initial conditions, not just those from the shortcut method, to ensure that the optimal values shown are indeed optimal and not influenced by the initial values.

Looking at the two key design and operating variables, the total number of stages and reflux ratio, the maximum deviations are 9% and 19%, respectively. This means that when setting the bounds in the optimisation using the shortcut values as initialisation, the bound can be narrowed to, e.g. ±25%, which can also reduce the computational burden and ease the convergence difficulty of the optimisation problem. For the other variables (e.g. F_{sl} and F_{sv}) from the shortcut method, they also show good agreements with the corresponding optimal designs, but note that these variables may be highly affected by the definition of the objective function and the cost equations considered in the optimisation. Thus, during optimisation, it is suggested to provide wider bounds for these variables based on the values from the proposed shortcut method.

The shortcut design is very close to the optimal design considering both the product purities and TACs, which further illustrates the effectiveness of the proposed shortcut method. The optimisation takes about 30-60 min, which is very quick for such a complex system. By taking the shortcut designs as the initial values, the rate of the infeasible simulations in each generation in the GA process is low for all case studies, which shows that the proposed shortcut method can help with the convergence of both simulations and optimisation.

5. Conclusion

In this work, a new shortcut method has been proposed which can be used for both simple and complex distillation column structures to obtain an initial estimate of all main design variables. The method is based on simple mass balances and the key concept of the method is to minimise energy, meaning that the main priority is to achieve pinch conditions in the design. The method can handle any constraints imposed by the different structures and, unlike other shortcut methods in the open literature, can solve the shortcut design problem simultaneously using a simple optimisation procedure without the need for iterative manual calculations. The proposed shortcut method can be easily adapted to any software, such as gPROMS, GAMS, Python, MATLAB, and even Excel. The shortcut design variables obtained can be used to initialise rigorous simulation or optimisation problems, thus greatly reducing the risk of initialisation failure or convergence issues.

The method is illustrated by four case studies: a simple conventional binary distillation column to explain and illustrate the method, then a ternary dividing wall column (DWC) as well as two modified DWC structures based on reduced vapour transfer (RVT-DWC). The DWC design is also compared to a rigorously optimised design, showing that the shortcut design is quite close to the optimal design, and that no convergence issues were experienced. It should be noted that the current shortcut method cannot yet be applied for azeotropic mixtures, and future work will be focused on the modification of the current shortcut method to also handle such systems.

Appendix A. Flash calculations

A flash calculation can be used to obtain the vapour and/or liquid composition of a mixture at a given temperature and pressure, or to obtain the bubble/dew point of the mixture at a given composition and pressure. The saturated vapour pressure of a component i, $P_{sat,i}$ (Pa), can be obtained from the Antoine equation (Perry and Green, 2008):

$$\ln(P_{sat,i}) = C_{1,i} + \frac{C_{2,i}}{T} + C_{3,i} \times \ln(T) + C_{4,i} \times T^{C_{5,i}} \quad \forall i = 1, \ldots, N_c \tag{A.1}$$

where $C_{1,i}$ to $C_{5,i}$ are the Antoine parameters for component i obtained from Perry and Green (2008) and T is the temperature (K).

The Raoult's Law states that the partial pressure of component i, p_i (Pa) can be described with:

$$p_i = x_i \times P_{sat,i} \quad \forall i = 1, \ldots, N_c \tag{A.2}$$

where x_i is the liquid molar composition of component i (mol mol^{-1}).

According to Dalton's Law:

$$p_i = y_i \times P \quad \forall i = 1, \ldots, N_c \tag{A.3}$$

where y_i is the vapour molar composition of component i (mol mol^{-1}), and P is the total pressure of the system (Pa).

The K-values of component i, K_i, can be obtained by substituting in the Dalton's and Raoult's Laws:

$$K_i = \frac{y_i}{x_i} = \frac{P_{sat,i}}{P} \quad \forall i = 1, \ldots, N_c \tag{A.4}$$

For the bubble point calculation (saturated liquid), the following equation should be satisfied:

$$\sum_{i=1}^{N_c} (K_i \times x_i) = 1 \tag{A.5}$$

For the dew point calculation (saturated vapour), the following equations should be satisfied:

$$\sum_{i=1}^{N_c} \frac{y_i}{K_i} = 1 \tag{A.6}$$

Appendix B. Full shortcut model of dividing wall column

The definitions of reflux ratio (RR^{main}), liquid split ratio (R_{sl}), and vapour split ratio (R_{sv}) in the main column are given as:

$$RR^{main} = \frac{F_9}{F_{d2}} \tag{B.1}$$

$$R_{sl} = \frac{F_1}{F_{10}} \tag{B.2}$$

$$R_{sv} = \frac{F_5}{F_{18}} \tag{B.3}$$

The mass balances to define all the streams are then:

$$F_{feed,L} = F_{feed} \times q \tag{B.4}$$

$$F_{feed,V} = F_{feed} \times (1 - q) \tag{B.5}$$

$$F_{d2} = F_{feed} \times z_A \tag{B.6}$$

$$F_s = F_{feed} \times z_B \tag{B.7}$$

$$F_{b3} = F_{feed} \times z_C \tag{B.8}$$

$$F_2 = F_1 \tag{B.9}$$

$$F_3 = F_2 + F_{feed,L} \tag{B.10}$$

$$F_4 = F_3 \tag{B.11}$$

$$F_6 = F_5 \tag{B.12}$$

$$F_7 = F_6 + F_{feed,V} \tag{B.13}$$

$$F_8 = F_7 \tag{B.14}$$

$$F_{10} = F_9 \tag{B.15}$$

$$F_{11} = F_{10} - F_1 \tag{B.16}$$

$$F_{12} = F_{11} \tag{B.17}$$

$$F_{13} = F_{12} - F_s \tag{B.18}$$

$$F_{14} = F_{13} \tag{B.19}$$

$$F_{15} = F_4 + F_{14} \tag{B.20}$$

$$F_{16} = F_{15} \tag{B.21}$$

$$F_{17} = F_{16} - F_{b3} \tag{B.22}$$

$$F_{18} = F_{17} \tag{B.23}$$

$$F_{19} = F_{18} - F_5 \tag{B.24}$$

$$F_{20} = F_{19} \tag{B.25}$$

$$F_{21} = F_{20} \tag{B.26}$$

$$F_{22} = F_8 + F_{21} \tag{B.27}$$

$$F_{23} = F_{22} \tag{B.28}$$

$$F_{d1} = F_8 - F_1 \tag{B.29}$$

$$F_{b1} = F_4 - F_5 \tag{B.30}$$

According to the assumption of pinch conditions, the following equations are fulfilled when considering a ternary mixture of components *A*, *B* and *C*, with *A* the lightest and *C* the heaviest component:

$$x_{tc1,i} = x_{1,i} = x_{10,i} = x_{11,i} \quad i \in \{A, B, C\} \tag{B.31}$$

$$y_{tc1,i} = y_{8,i} = y_{21,i} = y_{22,i} \quad i \in \{A, B, C\} \tag{B.32}$$

$$x_{tc2,i} = x_{4,i} = x_{14,i} = x_{15,i} \quad i \in \{A, B, C\} \tag{B.33}$$

$$y_{tc2,i} = y_{5,i} = y_{18,i} = y_{19,i} \quad i \in \{A, B, C\} \tag{B.34}$$

The number of stages in each column section can be calculated by the Fenske's equation:

$$N_{min} = \frac{\ln\left[\left(\frac{x_{lk}}{x_{hk}}\right)_D / \left(\frac{x_{lk}}{x_{hk}}\right)_B\right]}{\ln(\alpha_{lk-hk})} \tag{B.35}$$

When calculating the number of stages for *C2* and *C3*, *C2* and *C3* are considered as two separated columns separating a binary mixture of *AB* and *BC*, respectively. Thus the liquid compositions (x_{12} and x_{13}) can be considered as:

$$x_{12} = (x_{12,A}, x_{12,B}, x_{12,C}) = (1 - x_{spec,B}, x_{spec,B}, 0) \tag{B.36}$$

$$x_{13} = (x_{13,A}, x_{13,B}, x_{13,C}) = (0, x_{spec,B}, 1 - x_{spec,B}) \tag{B.37}$$

The component mass balances for the top thermal coupling location (*tc1*) are given by:

$$\alpha_{AB} = \frac{y_{tc1,A}/x_{tc1,A}}{y_{tc1,B}/x_{tc1,B}} \tag{B.38}$$

$$x_{tc1,C} = 0 \tag{B.39}$$

$$y_{tc1,C} = 0 \tag{B.40}$$

$$F_{feed} \times z_A = F_8 \times y_{tc1,A} - F_1 \times x_{tc1,A} \tag{B.41}$$

$$\sum_{i \in S_c} (y_{tc1,i}) = 1 \quad S_c = \{A, B, C\} \tag{B.42}$$

$$\sum_{i \in S_c} (x_{tc1,i}) = 1 \quad S_c = \{A, B, C\} \tag{B.43}$$

The component mass balances for the bottom thermal coupling location (*tc2*) are given by:

$$\alpha_{BC} = \frac{y_{tc2,B}/x_{tc2,B}}{y_{tc2,C}/x_{tc2,C}} \tag{B.44}$$

$$x_{tc2,A} = 0 \tag{B.45}$$

$$y_{tc2,A} = 0 \tag{B.46}$$

$$F_{feed} \times z_C = F_4 \times x_{tc2,C} - F_5 \times y_{tc2,C} \tag{B.47}$$

$$\sum_{i \in S_c} (y_{tc2,i}) = 1 \quad S_c = \{A, B, C\} \tag{B.48}$$

$$\sum_{i \in S_c} (x_{tc2,i}) = 1 \quad S_c = \{A, B, C\} \tag{B.49}$$

If the liquid composition of stream 10 ($x_{tc1,i}$) is assumed to be correct then the vapour composition of stream 22 ($y_{tc1,i}^{C2,top}$) can be calculated by performing the component mass balance around the top section of column *C2*. A similar procedure can also be applied to calculate the vapour composition of stream

18 ($y_{tc2,i}^{C3,bot}$). The equations are as below:

$$y_{tc1,i}^{C2,top} = \frac{F_{11} \times x_{11,i} + F_{23} \times y_{23,i} - F_9 \times x_{9,i}}{F_{22}} \quad i \in \{A, B, C\} \tag{B.50}$$

$$y_{tc2,i}^{C3,bot} = \frac{F_{15} \times x_{15,i} + F_{17} \times y_{17} - F_{16} \times x_{16,i}}{F_{18}} \quad i \in \{A, B, C\} \tag{B.51}$$

The deviation of the vapour composition of the thermal coupling streams can be determined from:

$$\Delta_{tc1}^{C2,top} = |y_{tc1,A} - y_{tc1,A}^{C2,top}| \tag{B.52}$$

$$\Delta_{tc2}^{C3,bot} = |y_{tc2,C} - y_{tc2,C}^{C3,bot}| \tag{B.53}$$

The vapour compositions of components *A* and *C* at the feed location can be calculated from the component balances around *C1 top* and *C1 bot*, respectively. Rearranging the component balances gives:

$$y_{feed,A}^{C1,top} == \frac{F_2 \times x_{2,i} + F_8 \times y_{8,i} - F_1 \times x_{1,i}}{F_7} \quad i \in \{A, B, C\} \tag{B.54}$$

$$y_{feed,C}^{C1,bot} == \frac{F_3 \times x_{3,i} + F_5 \times y_{5,i} - F_4 \times x_{4,i}}{F_6} \quad i \in \{A, B, C\} \tag{B.55}$$

The pinch variable for the feed pinch condition is calculated as:

$$\Delta_{feed} = |y_{feed,A} - y_{feed,A}^{C1,top}| + |y_{feed,C} - y_{feed,C}^{C1,bot}| \tag{B.56}$$

After applying the Fenske's equation of each column section, the pinch stage variable for the stage difference across the DWC wall is straight forward:

$$\Delta_N = |(N_{min}^{C1,top} + N_{min}^{C1,bot}) - (N_{min}^{C2,bot} + N_{min}^{C3,top})| \tag{B.57}$$

The objective function takes into account deviations in feed composition pinch, as well as the stage pinch for the DWC, and is defined:

$$Z = (\Delta_{feed} + 1) \times (\Delta_{tc1}^{C2,top} + 1) \times (\Delta_{tc2}^{C3,bot} + 1) \times (\Delta_N{}^2 + 1) \tag{B.58}$$

Appendix C. Dimension and cost equations

C.1 Dimension equations

In this section, equations of column design (shell and tray) are described based on the equations in Seider et al. (2016). The results from the shortcut method are compared with those of rigorous simulations based on a total annualised cost (TAC) optimisation. gPROMS ProcessBuilder can yield the values of internal column diameter and height of the column if the build-in column geometry function is activated so these two values are collected from the gPROMS ProcessBuilder results and used in the other user-defined equations. More details about the equations for calculating column internal diameter and column height can be found in the gPROMS ProcessBuilder documentation (Process Systems Enterprise, 2020).

Table 8 – Minimum wall thickness corresponding to the column inside diameter (Seider et al., 2016).

Column internal diameter (ft)	Minimum wall thickness, t_{min} (in.)
0–4	1/4
4–6	5/16
6–8	3/8
8–10	7/16
10–12	1/2

The cost equations for calculating the capital expenditure of a column (shell) requires the value of column shell weight, W_{shell} (lb) (Seider et al., 2016):

$$W_{shell} = \pi(D_i + t_s)(L + 0.8D_i)t_s\rho_{shell} \tag{C.1}$$

where D_i is column internal diameter (in.), t_s is average shell thickness (in.), L is column height (in.), and ρ_{shell} is density of column shell material (lb in.$^{-3}$).

Column design pressure, P_d (psig), is required for calculating t_s and must be higher than the column operating pressure, P_o (psig) (Seider et al., 2016):

$$P_d = 10 \quad 0 < P_o < 5 \tag{C.2}$$

$$P_d = e^{(0.60608+0.91615(\ln(P_o))+0.0015655(\ln(P_o))^2)} \quad 10 < P_o < 1000 \tag{C.3}$$

$$P_d = 1.1P_o \quad 1000 < P_o \tag{C.4}$$

The shell thickness, t_p (in.), required to withstand the internal pressure can be calculated (Seider et al., 2016):

$$t_p = \frac{P_d D_i}{2SE - 1.2P_d} \tag{C.5}$$

where *S* is maximum allowable stress (psi) with value as 15,000 and *E* is fractional weld efficiency with value as 0.85. The values set for *S* and *E* are default values in gPROMS ProcessBuilder.

As described by Seider et al. (2016), sometimes the calculated value of t_p is too small for low pressures, which cannot provide enough rigidity. Thus a minimum wall thickness is essential for such situations and the value of minimum wall thickness can be found by referring to Table 8 with the corresponding column internal diameter.

Another necessary wall thickness considered to withstand earthquake or wind at the column bottom, t_w (in.), is given by (Seider et al., 2016):

$$t_w = \frac{0.22(D_o + 18)L^2}{SD_o^2} \tag{C.6}$$

where D_o is the outer column diameter (in.) which is assumed to be the same as D_i following the assumption used by gPROMS ProcessBuilder.

Thus the average column wall thickness, t_s (in.), is given by (Seider et al., 2016):

$$t_s = MAX(t_p, t_{min}) + \frac{t_w}{2} \tag{C.7}$$

For DWC, two column sections are considered in the design as for design purposes the DWC is assumed to be equivalent

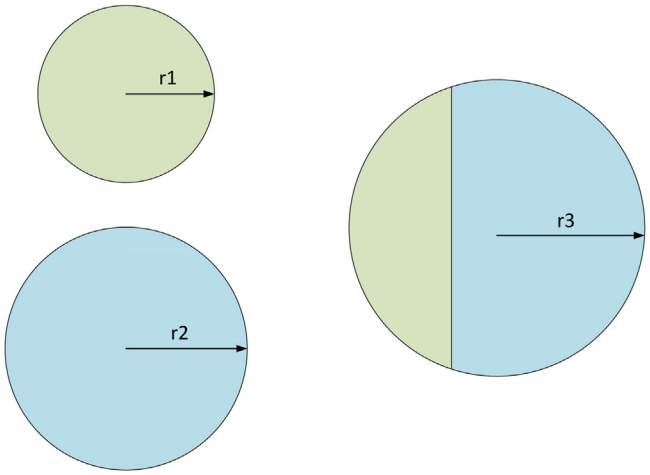

Fig. C1 – Tray dimension of Petlyuk and DWC structures.

to a Petlyuk design, however, this is not accurate when considering the capital expenditure as the DWC column diameter is not the summation of the two Petlyuk diameters. Thus a more accurate representation is to rearrange the Petlyuk design into one column section by considering the area of the actual DWC section as the summation of the areas of the two Petlyuk column sections. Fig. C1 shows how this method is achieved. The variables r_1 and r_2 are the radii of the prefractionator and the main column (m), respectively. Thus the radius of the DWC is assumed to be calculated by:

$$r_3 = \sqrt{r_1^2 + r_2^2} \tag{C.8}$$

This strategy is applied for the RVT-DWC designs as well. In addition, the height of the rearranged DWC is taken as the height of the main column in the Petlyuk design.

C.2 Cost equations

In this section, the cost equations of the distillation column are provided by Sinnott and Towler (2020). The objective function utilised in the rigorous optimisation is chosen as the commonly used total annualised cost, TAC ($\$\,y^{-1}$):

$$TAC = \frac{CAPEX_{total}}{t_{payback}} \times \frac{CEPCI_{2019}}{CEPCI_{2007}} + OPEX_{total} \tag{C.9}$$

where $t_{payback}$ is assumed as eight years, $CAPEX_{total}$ is the summation of all equipment capital expenditure, $OPEX_{total}$ is the summation of all operating costs, $CEPCI_{2007}$ is 509.7 (Sinnott and Towler, 2020) and $CEPCI_{2019}$ is 607.5 (Jenkins, 2020).

The cost of the distillation column vessel, $CAPEX_{shell}$ ($), includes the capital cost of shell and trays. The shell (stainless steel) cost is given by (Sinnott and Towler, 2020):

$$CAPEX_{shell} = f_{lang}(15000 + 68\,W_{shell}^{0.85}) \tag{C.10}$$

where f_{lang} is the Lang factor with value of 4.

The tray cost, $CAPEX_{tray}$ ($), is (Sinnott and Towler, 2020):

$$CAPEX_{tray} = 110 + 380 D_i^{1.8} \tag{C.11}$$

The capital cost of all trays, $CAPEX_{trays}$ ($), is (Sinnott and Towler, 2020):

$$CAPEX_{trays} = f_m N_{trays} CAPEX_{tray} \tag{C.12}$$

where f_m is a material factor, and for stainless steel the value is 1.3 (Sinnott and Towler, 2020). N_{trays} is the total number of trays in a column excluding the reboiler and condenser.

Another main contribution to capital expenditure comes from the reboiler, $CAPEX_R$ ($) (Sinnott and Towler, 2020):

$$CAPEX_R = f_{lang} f_m (25000 + 340 A_R^{0.9}) \tag{C.13}$$

where A_R is the heat exchanger area (m^2) of the reboiler (Luyben, 2013):

$$A_R = \frac{Q_R}{\Delta T_R\, U_R} \tag{C.14}$$

where Q_R is the reboiler duty (kW), $\Delta T_R = 10\,K$, and $U_R = 0.75\,kW\,m^{-2}\,K^{-1}$ (Tsatse et al., 2021).

The capital cost of the condenser, $CAPEX_C$ ($), is also considered (Sinnott and Towler, 2020):

$$CAPEX_C = f_{lang} f_m (24000 + 46 A_C^{1.2}) \tag{C.15}$$

where A_C is the heat exchanger area (m^2) of the condenser (Luyben, 2013):

$$A_C = \frac{Q_C}{\Delta T_C\, U_C} \tag{C.16}$$

where Q_C is the condenser duty (kW), $\Delta T_C = 10\,K$, and $U_C = 0.75\,kW\,m^{-2}\,K^{-1}$ (Tsatse et al., 2021).

Therefore, the total capital cost is:

$$CAPEX_{total} = CAPEX_{shell} + CAPEX_{trays} + CAPEX_R + CAPEX_C \tag{C.17}$$

It should be noted that the cost for the wall (i.e. internal partitions) in a DWC is not taken into account.

The only operating cost considered is the cost of the heat utility, $OPEX_R$ ($\$\,y^{-1}$), and assuming this is steam (note that proper unit conversion should be applied):

$$OPEX_{total} = OPEX_R = Q_R Price_{steam} \tag{C.18}$$

where $Price_{steam} = 24\,€\,t^{-1}$, the operating time per year is taken as 8400 h, and the currency exchange is taken as $1.13\,\$\,€^{-1}$.

Declaration of Competing Interest

The authors report no declarations of interest.

References

Agrawal, R., 2000. Thermally coupled distillation with reduced number of intercolumn vapor transfers. AIChE J. 46 (11), 2198–2210.

Amminudin, K., Smith, R., 2001. Design and optimization of fully thermally coupled distillation columns. Chem. Eng. Res. Des. 79 (7), 716–724.

Aspen Technology Inc, 2017. Aspen Plus V10.

Bandyopadhyay, S., 2006. Extended Smoker's equation for calculating number of stages in distillation. In: Sorensen, E. (Ed.), Distillation and Absorption. IChemE, pp. 937–944.

Castillo, F.J.L., Thong, D.Y., Towler, G.P., 1998. Homogeneous azeotropic distillation. 1. Design procedure for single-feed columns at nontotal reflux. Ind. Eng. Chem. Res. 37 (3), 987–997.

Chia, D.N., Duanmu, F., Sorensen, E., 2021. Optimal design of distillation columns using a combined optimisation approach. In: Turkay, M., Gani, R. (Eds.), 31st European Symposium on

Computer Aided Process Engineering. Elsevier B.V., pp. 153–158.
Chou, S.-M., Yaws, C.L., Cheng, J.-S., 1986. Application of factor method for minimum reflux: multiple feed distillation columns. Can. J. Chem. Eng. 64 (2), 254–259.
Colburn, A.P., 1941. The calculation of minimum reflux ratio in the distillation of multi-component mixtures. Trans. Am. Inst. Chem. Engrs. 37, 805.
Dejanović, I., Matijašević, L., Olujić, Z., 2010a. Dividing Wall Column Application for Platformate Splitter – A Case Study., pp. 655–660.
Dejanović, I., Matijašević, L., Olujić, Z., 2010b. Dividing wall column – a breakthrough towards sustainable distilling. Chem. Eng. Process.: Process Intensif. 49 (6), 559–580.
Fenske, M.R., 1932. Fractionation of straight-run pennsylvania gasoline. Ind. Eng. Chem. 24 (5), 482–485.
Gani, R., Bek-Pedersen, E., 2000. Simple new algorithm for distillation column design. AIChE J. 46 (6), 1271–1274.
Gilliland, E.R., 1940. Multicomponent rectification estimation of the number of theoretical plates as a function of the reflux ratio. Ind. Eng. Chem. 32 (9), 1220–1223.
Glinos, K., Malone, M.F., 1984. Minimum reflux, product distribution and lumping rules for multicomponent distillation. Ind. Eng. Chem. Process Des. Dev. 23 (4), 764–768.
Halvorsen, I.J., 2001. Minimum Energy Requirements in Complex Distillation Arrangements (Ph.D. thesis). Norwegian University of Science and Technology.
Hengstebeck, R., 1946. A simplified method for solving multicomponent distillation problems. Trans. AIChE 42, 309–329.
Jafarey, A., Douglas, J.M., McAvoy, T.J., 1979. Short-cut techniques for distillation column design and control. 1. Column design. Ind. Eng. Chem. Process Des. Dev. 18 (2), 197–202.
Jenkins, S., 2020. 2019 Chemical Engineering Plant Cost Index Annual Average.
Kirkbride, C.G., 1944. Process design procedure for multicomponent fractionators. Petrol. Refiner 23 (9).
Kong, L., Maravelias, C.T., 2019. From graphical to model-based distillation column design: a McCabe–Thiele-inspired mathematical programming approach. AIChE J. 65 (11).
Lewis, W.K., 1909. The theory of fractional distillation. J. Ind. Eng. Chem. 1 (8), 522–533.
Luyben, W.L., 2013. Distillation Design and Control Using Aspen Simulation, 2nd ed. John Wiley & Sons, Hoboken, NJ, USA.
McCabe, W.L., Thiele, E.W., 1925. Graphical design of fractionating columns. Ind. Eng. Chem. 17 (6), 605–611.
Muralikrishna, K., Madhavan, V., Shah, S., 2002. Development of dividing wall distillation column design space for a specified separation. Chem. Eng. Res. Des. 80 (2), 155–166.
Perry, R.H., Green, D.W., 2008. Perry's Chemical Engineers' Handbook, Vol. 1. McGraw-Hill Book Company.
Process Systems Enterprise, 2019. gO:MATLAB.
Process Systems Enterprise, 2020. gPROMS ProcessBuilder Version 1.4.
Ränger, L.M., Grützner, T., 2021. Shortcut method for initialization of dividing-wall columns and estimating Pareto-optimal NQ-curves. Chem. Eng. Technol. 44 (10), 1919–1928.
Ramapriya, G.M., Tawarmalani, M., Agrawal, R., 2014. Thermal coupling links to liquid-only transfer streams: a path for new dividing wall columns. AIChE J. 60 (8), 2949–2961.
Seedat, N., Kauchali, S., Patel, B., 2020. Novel representation of vapour-liquid equilibrium curves for multicomponent systems: design of total reflux distillation columns. Chem. Eng. Res. Des. 155, 22–39.
Seider, W.D., Lewin, D.R., Seader, J.D., Widagdo, S., Gani, R., Ng, K.M., 2016. Product and Process Design Principles: Synthesis, Analysis and Evaluation, 4th ed. Wiley.
Sinnott, R., Towler, G., 2020. Chemical Engineering Design, 6th ed. Elsevier.
Skiborowski, M., Rautenberg, M., Marquardt, W., 2015. A hybrid evolutionary-deterministic optimization approach for conceptual design. Ind. Eng. Chem. Res. 54 (41), 10054–10072.
Smith, B., 1963. Design of Equilibrium Stage Processes. McGraw-Hill Book Company.
Smoker, E., 1938. Analytical determination of plates in fractionating columns. Trans. Am. Inst. Chem. Engrs. 34, 165.
Sorensen, E., 2014. Principles of binary distillation. In: Górak, A., Sorensen, E. (Eds.), Distillation: Fundamentals and Principles, chapter 4. Academic Press, Boston, pp. 145–185 (Chapter 4).
Sotudeh, N., Hashemi Shahraki, B., 2007. A method for the design of divided wall columns. Chem. Eng. Technol. 30 (9), 1284–1291.
Tedder, D.W., Rudd, D.F., 1978. Parametric studies in industrial distillation: Part I. Design comparisons. AIChE J. 24 (2), 303–315.
The MathWorks Inc, 2019. MATLAB R2019b Version 9.7.
Towler, G., Sinnott, R., 2007. Chemical Engineering Design – Principles, Practice and Economics of Plant and Process Design. Elsevier.
Triantafyllou, C., Smith, R., 1992. Design and optimisation of fully thermally coupled distillation columns. Chem. Eng. Res. Des. 70 (A2), 118–132.
Tsatse, A., Oudenhoven, S., ten Kate, A., Sorensen, E., 2021. Optimal design and operation of reactive distillation systems based on a superstructure methodology. Chem. Eng. Res. Des. 170, 107–133.
Underwood, A.J.V., 1949. Fractional distillation of multicomponent mixtures. Ind. Eng. Chem. 41 (12), 2844–2847.
Urselmann, M., Barkmann, S., Sand, G., Engell, S., 2011. A memetic algorithm for global optimization in chemical process synthesis problems. IEEE Trans. Evol. Comput. 15 (5), 659–683.
Van Dongen, D.B., Doherty, M.F., 1985. Design and synthesis of homogeneous azeotropic distillations. 1. Problem formulation for a single column. Ind. Eng. Chem. Fundam. 24 (4), 454–463.
Winn, W., 1958. New relative volatility method for distillation calculations. Petrol. Refiner 37 (5), 2–6.